THE JOURNAL OF BIOLOGICAL CHEMISTRY VOL. 282, NO. 5, pp. 3105–3121, February 2, 2007

A Comprehensive Structure-Function Map of the Intracellular Surface of the Human C5a Receptor

*I. IDENTIFICATION OF CRITICAL RESIDUES**[S]

Received for publication, August 11, 2006, and in revised form, November 17, 2006 Published, JBC Papers in Press, November 29, 2006, DOI 10.1074/jbc.M607679200

Marissa L. Matsumoto[‡], Kirk Narzinski[‡], Philip D. Kiser[‡], Gregory V. Nikiforovich[§], and Thomas J. Baranski[‡1]

From the [‡]Departments of Medicine and Molecular Biology & Pharmacology and the [§]Department of Biochemistry and Molecular Biophysics, Washington University School of Medicine, St. Louis, Missouri 63110

G protein-coupled receptors are one of the largest protein families in nature; however, the mechanisms by which they activate G proteins are still poorly understood. To identify residues on the intracellular face of the human C5a receptor that are involved in G protein activation, we performed a genetic analysis of each of the three intracellular loops and the carboxyl-terminal tail of the receptor. Amino acid substitutions were randomly incorporated into each loop, and functional receptors were identified in yeast. The third intracellular loop contains the largest number of preserved residues (positions resistant to amino acid substitutions), followed by the second loop, the first loop, and lastly the carboxyl terminus. Surprisingly, complete removal of the carboxyl-terminal tail did not impair C5a receptor signaling. When mapped onto a three-dimensional structural model of the inactive state of the C5a receptor, the preserved residues reside on one half of the intracellular surface of the receptor, creating a potential activation face. Together these data provide one of the most comprehensive functional maps of the intracellular surface of any G protein-coupled receptor to date.

G protein-coupled receptors (GPCRs)[2] are seven transmembrane (TM)-spanning proteins that play important roles in many diverse signaling processes, including olfaction, vision, taste, chemotaxis, and yeast cell mating. GPCRs activate signaling cascades by transmitting a signal to heterotrimeric G proteins composed of a Gα, Gβ, and Gγ subunit. Upon ligand binding, the GPCR acts as a guanine nucleotide exchange factor through a conformational change that is transmitted to Gα-GDP, leading to GTP exchange for GDP. Gα-GTP then dissociates from G$\beta\gamma$, and both Gα-GTP and G$\beta\gamma$ can transmit the signal to downstream effectors such as adenylyl cyclase, phospholipase C, mitogen-activated protein kinases, and ion channels. Activation of these second messengers can lead to a wide variety of physiological responses. GPCRs are one of the largest protein families in nature and are found in nearly all organisms from yeast to human. An estimated 1% of the human genome encodes GPCRs and ~30% of all pharmaceutical drugs target these receptors (1).

The GPCR family of proteins can be divided into three major subgroups based on sequence similarity (2). The largest subgroup is the rhodopsin-like family (class A), whose prototypical member, rhodopsin, is the only GPCR for which a crystal structure has been solved (3–7). This family of receptors is distinguished by a set of 20 highly conserved amino acids near the cytoplasmic side of the TM core. The DRY motif, found in this region at the TM3-second intracellular loop junction, is essential for G protein activation (8–10). The intracellular and extracellular loop regions of GPCRs within the same family contain the most sequence diversity. The extracellular loops presumably require distinct sequences to accommodate a diverse set of ligands. However, the reason for the lack of homology among intracellular loops of receptors that couple to similar G proteins, and presumably activate them through a similar mechanism, is less clear. This lack of homology makes it extremely difficult to use bioinformatics to predict residues required for signaling as well as the G protein(s) to which a given receptor may couple. Thus, a large scale genetic approach is necessary to understand G protein coupling and activation.

Despite intense focus on GPCRs it is still not known how they dock to G proteins and catalyze the exchange of GTP for GDP. A wide variety of techniques have been applied to the study of how GPCRs function as receptor switches for G protein binding and activation. These include peptide competition (11), cysteine or alanine scanning mutagenesis (12–18), deletion mapping (8), cross-linking (19, 20), intracellular loop swapping experiments (21–24), and random saturation mutagenesis targeting single intracellular loops (25–28). Although results differ depending on which GPCR is studied, the consensus is that intracellular loops 2 and 3 (IC2 and IC3) are critical for signal-

* This work was supported by American Heart Association Grant 06500BGZ (to T. J. B.), the Culpepper Award, the Rockefeller Brothers Fund (to T. J. B.), and National Institutes of Health Grants GM63720-01 (to T. J. B.) and GM068460 (to G. V. N.). The costs of publication of this article were defrayed in part by the payment of page charges. This article must therefore be hereby marked "*advertisement*" in accordance with 18 U.S.C. Section 1734 solely to indicate this fact.

[S] The on-line version of this article (available at http://www.jbc.org) contains supplemental Figs. S1 and S2.

[1] To whom correspondence should be addressed: Depts. of Medicine and Molecular Biology & Pharmacology, Washington University School of Medicine, Campus Box 8127, 660 S. Euclid Ave., St. Louis, MO 63110. Tel.: 314-747-3997; Fax: 314-362-7641; E-mail: baranski@wustl.edu.

[2] The abbreviations used are: GPCR, G protein-coupled receptor; 3AT, 3-amino-1,2,4-triazole; C5a, complement factor 5a; C5aR, complement factor 5a receptor; CT, carboxyl terminus; CT1, first half of the carboxyl terminus; CT2, second half of the carboxyl terminus; CXCR4, chemokine receptor 4; Endo-H_f, endo-β-*N*-acetylglucosaminidase H; ER, endoplasmic reticulum; IC1, intracellular loop 1; IC2, intracellular loop 2; IC3, intracellular loop 3; IP_3, inositol-1,4,5-triphosphate; m5R, m5 muscarinic acetylcholine receptor; r.m.s.d., root mean square deviation; RSM, random saturation mutagenesis; TM, transmembrane; W5Cha, hexapeptide agonist of the C5a receptor; YFP, yellow fluorescent protein.

Supplemental Material can be found at: http://www.jbc.org/cgi/content/full/M607679200/DC1

ing and that the DRY motif of rhodopsin-like receptors is essential (8–10).

To gain a more comprehensive understanding of the intracellular structural determinants that mediate GPCR signaling, we performed random saturation mutagenesis (RSM) screens targeting each of the individual intracellular loops (IC1, IC2, and IC3) as well as the carboxyl terminus (CT) of the human C5a receptor (C5aR). The C5aR, a member of the rhodopsin-like family, binds the 74-amino acid complement-derived C5a peptide and is involved in chemotaxis and activation of leukocytes. The C5aR exhibits 20% sequence identity and 35% sequence homology with bovine rhodopsin and has similarly sized loop regions, indicating that it may adopt a similar structure. We have previously used RSM to identify functional residues in the C5aR extracellular loops (29–31) and TM regions (32, 33). RSM is a powerful structure-function analysis tool, because it introduces many unbiased amino acid substitutions and allows one to infer the relative importance of each residue within a region judged by the ability of that position to tolerate mutations. This study provides one of the most comprehensive functional maps of the intracellular face of any GPCR. In addition, these data, combined with our previous RSM screens of the extracellular loops (29–31) and the TM regions (32, 33), gives a broad view of residues critical for signaling of the C5aR.

EXPERIMENTAL PROCEDURES

Library Construction and Site-directed Mutagenesis—Silent restriction sites were engineered at the approximate boundaries of the intracellular loops IC1 (MluI and NdeI), IC2 (PstI and SfiI), or IC3 (BspEI and HindIII) of the C5aR ORF cloned into the pBS-SK Bluescript vector. The carboxyl terminus was divided into two regions, CT1 (FseI and BspEI) and CT2 (BspEI and XbaI), because of its large size. To prevent contamination by wild-type receptor in the libraries, a piece of non-receptor DNA was inserted between MluI and NdeI for IC1 and PstI and SfiI for IC2, and premature stop codons were inserted into the IC3 loop and the CT1 and CT2 regions. The following oligonucleotides were used (Integrated DNA Technologies, Coralville, IA), where the underlined region denotes bases randomly doped at a 20% non-wild-type nucleotide substitution rate: IC1, 5′-TATAACGCGTTGGTTGTTTGGGTTACTGCTTTTGAAGCTAAAAGAACTATTAATGCCATATGG-3′; IC2, 5′-TATACTGCAGATCGTTTTCTACTAGTTTTTAAACCAATTTGGTGTCAAAATTTTCGTGGGGCCGGCTTGGCCAAG-3′; IC3, 5′-TATATCCGGACTTGGTCTAGAAGAGCTACTAGATCTACTAAAACTTTGAAAGTTGTTGTTGCTGTTGTTGCAAGCTTG-3′; CT1, 5′-ATAGTGGCCGGCCAAGGTTTTCAAGGTAGATTGAGAAAATCTTTGCCATCTTTGCTCCGGAG-3′; and CT2, 5′-ATACTCCGGAATGTTTTGACTGAAGAATCTGTTGTTAGAGAATCTAAATCTTTTACTAGATCTACTGTTGATACTATGGCTCAAAAAACTCAAGCTGTCTAGACA-3′. Oligonucleotides were mutually primed by palendromic sequences at their 3′-ends, and complementary sequences were generated by Klenow extension. The double-stranded regions were then cut with the appropriate restriction enzymes and subcloned into the C5aR gene in the pBS-SK Bluescript vector. The complexity and quality of the libraries were then determined by sequencing ten unselected receptors. The mutant receptors were subsequently subcloned into an *ADE2* yeast expression vector. Single point mutations were made by designing complementary oligonucleotides encoding the desired mutation. A two-step PCR strategy was used to introduce the point mutation into the wild-type C5aR coding sequence in an *ADE2* yeast expression vector. YFP-tagged receptors were made by subcloning point mutations into a C5aR-YFP fusion construct containing YFP at the carboxyl terminus. All point mutations were confirmed by sequencing at the Washington University Protein and Nucleic Acid Chemistry Laboratory. The *RGS4* plasmid was a gift from Dr. Maurine Linder.

Yeast Strains—The *Saccharomyces cerevisiae* strain BY1142 has been previously described (32). Briefly, the genotype is *MATα far1Δ1442 tbt1-1 fus1::P_{FUS1}-HIS3 can1 ste14::trp1::LYS2 ste3Δ1156 gpa1* (41)-Gα_{i3} *lys2 ura3 leu2 trp1 his3 ade2*. This strain, modified from CY1141 (34), expresses a fusion of the amino-terminal 41 amino acids of the yeast Gα protein, Gpa1, followed by residues 34–354 of human Gα_{i3}. Activation of the C5aR leads to signaling through the mitogen-activated protein kinase cascade and expression of the P_{FUS1}-*HIS3* reporter gene, allowing the yeast to grow in the absence of histidine. The BY1143 strain was created by transforming the BY1142 strain with a *URA3* plasmid encoding C5a (pBN444) as previously described (29, 32). The BY1144 strain was created by transforming the BY1142 strain with an empty *URA3* vector (pBN443). BY1173 has the genotype *MATa ura3 leu2 trp1 his3 can1 gpa1Δ::ade2Δ::3XHA far1Δ::ura3Δ fus1Δ::P_{FUS1}-HIS3 LEU2::P_{FUS1}-lacZ sst2Δ::ura3Δ ste2Δ::G418R trp1::GPA1/*Gα_{i3} and has been previously described (35). BY1173 contains a fusion of amino acids 1–467 of the yeast Gα protein, Gpa1, followed by the last 5 amino acids of human Gα_{i3}. Activation of the C5aR leads to expression of a P_{FUS1}-β-galactosidase reporter gene.

Yeast Transformation and Functional Receptor Selection—Yeast transformations were done according to standard lithium acetate or electroporation protocols. Mutant receptors were screened by transforming BY1143 with the various *ADE2* mutant libraries and plating on non-selective medium for 1 day. Functional receptors were then selected by replica plating onto histidine-deficient medium containing either 5 mM 3-amino-1,2,4-triazole (3AT) (Sigma) for IC1, IC2, and IC3 or 100 mM 3AT for the CT1 and CT2 libraries. The higher concentration of 3AT was used for the carboxyl terminus to try to isolate receptors that signal at a high level, because many mutations were tolerated in this region. Receptor-encoding plasmids were recovered from the yeast and retested for signaling by retransforming into BY1143. Approximately 30 functional receptors were selected in each screen, because this number has been shown to be sufficient to determine critical residues (29, 30, 32, 33). Relative signaling abilities were assayed by restreaking three transformants of each mutant onto histidine-deficient medium containing varying amounts of 3AT (0, 1, 5, 10, 20, and 50 mM). Signaling levels were compared with wild-type C5aR expressed from an *ADE2* plasmid, pBN482 (grows on up to 5 mM 3AT), and a non-functional mutant C5aR containing a stop codon in TM3, pBN483 (does not grow on 1 mM 3AT), which were previously described (32, 33). Growth in the absence of

histidine was inferred to be dependent on C5aR signaling based on colony color (red colonies lack the C5aR *ADE2* plasmid). Plasmids encoding functional receptors were sequenced at the Washington University Protein and Nucleic Acid Chemistry Laboratory. All functional mutants were assessed for constitutive activity by expressing them in BY1144, which lacks a ligand, and replica plating on varying amounts of 3AT (0, 1, 5, 10, 20, and 50 mM).

Receptor Expression Levels—Expression levels of RSM mutants and single point mutants were determined by Western blot. Overnight cultures of yeast carrying an empty *ADE2* vector, or pBN482 encoding the wild-type C5aR, or plasmids encoding mutants were grown in liquid synthetic dropout medium-Ade. The A_{600} was determined and cultures were adjusted to $A_{600} = 10.0$. Cells harvested from 1 ml of adjusted cultures were lysed in 200 μl of 1× sample buffer (50 mM Tris-Cl, pH 6.8, 2% SDS, 10% glycerol supplemented with 2% β-mercaptoethanol, 1 μg/ml leupeptin, 1 μg/ml aprotinin, and 500 μM phenylmethylsulfonyl fluoride) with glass beads by vortexing for 5 min at room temperature. Lysates were heated for 5 min at 50 °C. 25 μl of each lysate was resolved on a 12% SDS-PAGE gel, transferred to polyvinylidene difluoride, and immunoblotted with a rabbit polyclonal anti-C5aR antibody raised against residues 9–29 of the amino terminus. Blots of YFP-tagged receptors were immunoblotted instead with a rabbit polyclonal anti-GFP antibody (Santa Cruz Biotechnology, Santa Cruz, CA). All blots were then stripped in 0.2 N NaOH for 15 min at room temperature, washed, and probed with a mouse monoclonal anti-β-actin antibody (AbCam) as a loading control.

Fluorescent Microscopy—BY1142-expressing YFP-tagged receptors was grown in liquid culture overnight, and live yeast were placed on a microscope slide. Images were recorded using a Zeiss color AxioCam HRc mounted on a Zeiss Axioscope microscope equipped with a Zeiss CP-Achromat 100× objective using a standard fluorescein isothiocyanate filter set.

β-Galactosidase Assays—BY1173 was transformed with wild-type or single point mutant receptors and treated with a range of concentrations (10^{-10} M to 10^{-5} M) of the C5aR hexapeptide agonist W5Cha (Genscript), which unlike C5a can cross the yeast cell wall. Three independent transformants were used for each receptor, and assays were performed in triplicate as previously described (29).

Endo-β-N-acetylglucosaminidase Treatment and Western Blots—Single point mutants that showed impaired signaling in the yeast system were subcloned into pcDNA3.1(+) (Invitrogen) and transiently transfected into HEK293 cells by standard calcium phosphate methods. Cells were lysed 2 days after transfection in 250 μl of 1× sample buffer (50 mM Tris-Cl, pH 6.8, 2% SDS, 10% glycerol) supplemented with 2% β-mercaptoethanol, 1 μg/ml leupeptin, 1 μg/ml aprotinin, and 500 μM phenylmethylsulfonyl fluoride by shearing through a 27-gauge syringe. Lysates were heated for 5 min at 50 °C. 27 μl of each lysate was treated with 1000 units of endo-β-*N*-acetylglucosaminidase H-maltose-binding protein fusion (Endo-H_f, New England Biolabs) at 37 °C for 3 h. Samples were heated for 5 min at 50 °C, resolved on a 12% SDS-PAGE gel, transferred to polyvinylidene difluoride, and immunoblotted with a rabbit polyclonal anti-C5aR antibody raised against residues 9–29 of the amino terminus. Blots were then stripped in 0.2 N NaOH for 15 min at room temperature, washed, and probed with a mouse monoclonal anti-β-actin antibody (AbCam) as a loading control.

Inositol 1,4,5-Triphosphate Accumulation—Single point mutants in pcDNA3.1(+) (Invitrogen) and human $G\alpha_{16}$ in pcDNA3.1(+) were transiently co-transfected into HEK293 cells. Cells were treated with 0.1 μM or 1 μM W5Cha (GenScript) or no ligand, and IP_3 levels were measured as previously described (29). Statistical significance was determined using a one-way analysis of variance test with Dunnett's post test and a 95% confidence level (GraphPad).

Molecular Modeling—Generally, molecular modeling procedures were as described earlier (36). All loops were mounted on the "template," *i.e.* on a three-dimensional structure of the TM region of C5aR based on the x-ray structure of rhodopsin (PDB entry 1F88). TM helical fragments of C5aR were defined by sequence homology to the rhodopsin helices found by the ClustalW procedure (ca.expasy.org/tools) as follows: TM1, Ile^{38}–Val^{50}–Ala^{63} (the first, middle, and last residues, respectively); TM2, Asn^{71}–Leu^{84}–Gln^{98}; TM3, Ala^{107}–Ala^{122}–Val^{138}; TM4, Ala^{150}–Trp^{161}–Phe^{172}; TM5, Glu^{199}–Phe^{211}–Phe^{224}; TM6, Arg^{236}–Phe^{251}–Phe^{267}; and TM7, Leu^{281}–Tyr^{290}–Tyr^{300}. The helical fragments were assembled into a TM helical bundle by following the procedure of "enhanced homology modeling" previously described in detail (37, 38). All energy calculations were performed using the ECEPP/2 force field with rigid valence geometry (39, 40). Only *trans* conformations of Pro residues were considered, and residues Arg, Lys, Glu, and Asp were present as charged species.

Geometrical sampling of the individual loops was performed from the smallest loop to the largest, *i.e.* from IC1 to IC2 to IC3. As soon as the resulting structures of the smaller loops were selected, the loop structure closest to the average spatial positions of the Cα atoms was included in the template, providing additional geometrical limitations for the larger loops. The sampling was, basically, a stepwise elongation of the loop covering all combinations of the possible backbone conformations for the stepwise growing loops, *i.e.* fragments 63–71 (IC1), 138–150 (IC2), 224–236 (IC3), and 300–310, the latter fragment representing the "minimal-length" carboxyl terminus as was found by the carboxyl-terminal screen (Fig. 6). Starting conformations of individual residues and overall sampling procedure were as described earlier (36) with limitations on the residue-residue contacts within the loop (Cα–Cα distances ≥4 Å), on the contacts between the loop and the template (Cα–Cα distances ≥6 Å); the values of coefficients EL and DEL were 3.0 and 0.0, respectively (see Ref. 36). Elongation steps were as follows: a single step from residue 60 to residue 74 for IC1; from 138 to 146 to 148 to 150 for IC2, from 224 to 232 to 234 to 236 for IC3, and from 300 to 310 for the last fragment.

After geometrical sampling selected all potentially loop-closing conformations for a specific loop, the selected structures were subjected to energy minimization employing the ECEPP/2 force field; the dielectric constant was set at 80 to mimic to some extent the water environment of the protruding loops. All parameters employed for energy minimization were as described previously (36). Energy calculations yielded 23 low

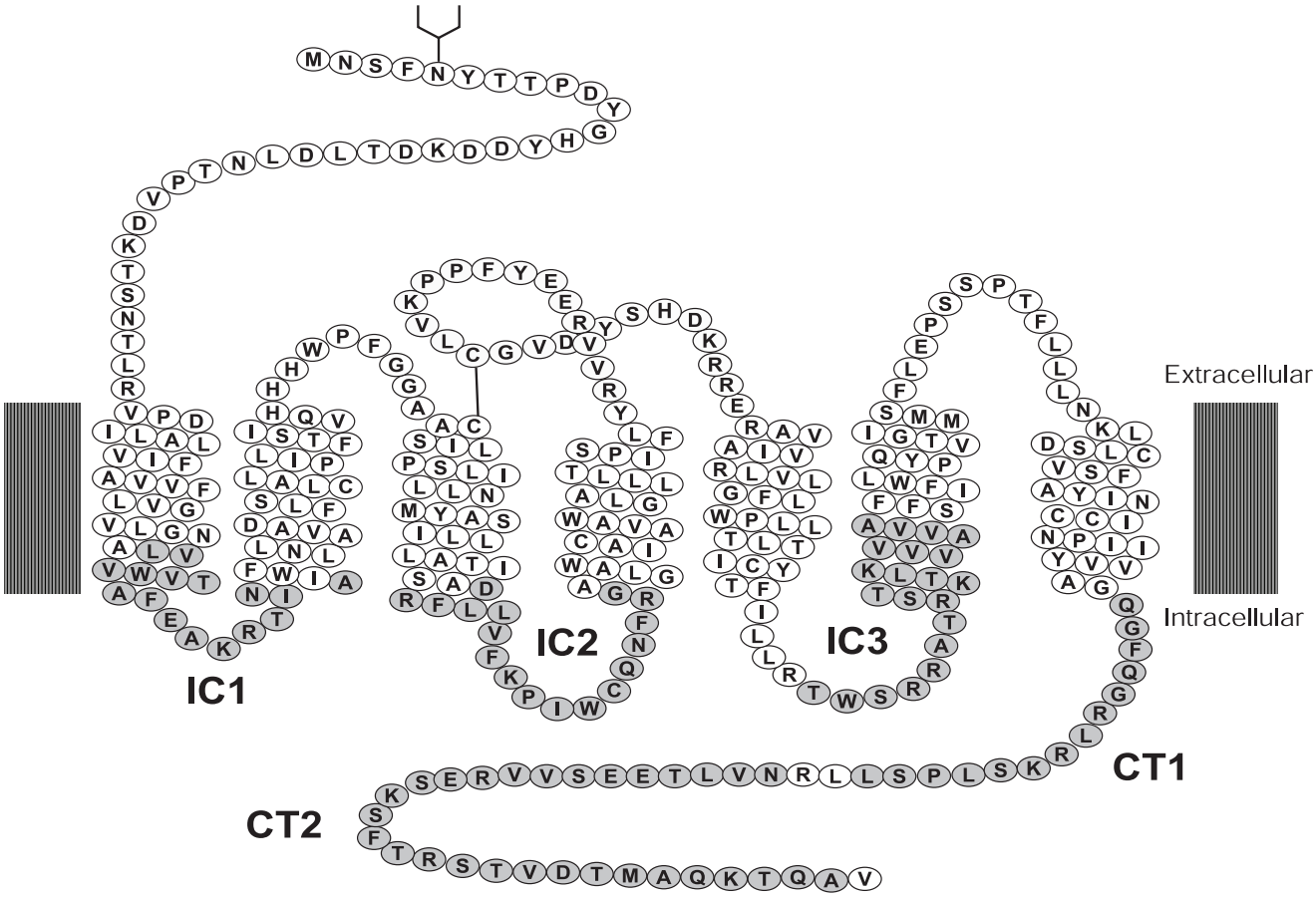

FIGURE 1. **Schematic of the human C5a receptor.** Residues targeted in the individual screens are shaded in *gray*: IC1 (57–72), IC2 (133–149), IC3 (229–249), CT1 (305–318), and CT2 (321–349). An *N*-linked glycosylation site is shown as a *stick figure*, and the lipid bilayer is depicted as *gray rectangles*.

energy structures (those with relative energy $\Delta E = E - E_{min} \leq$ 10 kcal/mol), which formed a single cluster of similar structures (defined by an r.m.s.d. value of ≤2 Å, Cα atoms only) for IC1; 90 structures within $\Delta E \leq 18$ kcal/mol falling into 21 different clusters for IC2; 25 structures within $\Delta E \leq 12$ kcal/mol falling into 3 different clusters for IC3; and 3 clusters for possible spatial arrangements of fragment 300–310. The elevated energy cut-off for IC2 was used to compensate for an energy gap of ~6 kcal/mol between the lowest energy structure and the second lowest energy one, which otherwise might cause a drastic decrease of the number of selected low energy conformations. The lowest energy conformers in each cluster were selected as representatives for further consideration in the intracellular package comprising all combinations of conformations for IC1 + IC2 + IC3 + fragment 300–310 (189 combinations). Then, for all combinations of representatives, energy calculations were performed with the same limitations as those described earlier (36). Fifty-six combinations were finally selected by an energy cut-off of 30 kcal/mol; they were divided into 16 clusters with different structures of IC1 + IC2 + IC3 according to the r.m.s.d. cut-off of 2 Å (Cα atoms only).

RESULTS

Identification of Functional Mutant Receptors—To identify residues that mediate signaling in the C5aR, RSM was used to introduce a large number of unbiased mutations into the IC1, IC2, and IC3 regions, as well as the carboxyl terminus (Fig. 1). The boundaries of the regions mutated were chosen by the ability to insert unique, silent restriction sites. Only the second half of IC3 is targeted in this study, because the first half was included in the TM5 screen (32). Because the maximum number of amino acids that can be scanned by RSM is 25–30 amino acids, the first half (CT1) and the second half (CT2) of the carboxyl terminus were targeted individually. Libraries of mutant receptors were made for each region separately by using oligonucleotides synthesized with a 20% non-wild-type nucleotide substitution rate. Previous studies have shown that this mutation rate leads to receptors with approximately a 35% amino acid substitution rate in the targeted regions (29, 30, 32, 33). Such a high mutation rate allows us to identify important residues judged by their inability to tolerate mutations. Libraries were made for each region, and ten unselected receptors were sequenced to determine the quality and complexity of the libraries (Table 1). An amino acid mutation rate of 35–38% was obtained for each library.

To screen a large number of mutant receptors, we took advantage of the ability to assay for functional C5aRs in *S. cerevisiae*. This system allows us to study signaling of a single GPCR through a single G protein in the absence of other competing receptors and G proteins. In addition, the yeast system lacks many receptor-interacting proteins such as GPCR kinases

TABLE 1

Characteristics of libraries and functional receptors

Data for the unselected libraries and for the selected functional receptors are shown: size, number of independent colony forming units in each loop library; AA Scanned, number of amino acids in each loop targeted by mutagenesis; AAΔ, average number of amino acid substitutions per recombinant and the rate of substitution, shown in parentheses. Preserved residues is as defined in the text.

Loop	Libraries			Selected receptors		
	Size ($\times 10^3$)	AA[a] scanned	AAΔ	No. receptors	AAΔ	Preserved residues
IC1	175	16	ND[b]	28	4.6 (29%)	2
IC2	100	17	6.5 (38%)	30	4.1 (28%)	6
IC3	737	21	8.0 (38%)	18	2.9 (14%)	11
CT1	7000	14	4.9 (35%)	14 FL 13 Trunc[c]	4.9 (35%)	1
CT2	700	29	10.2 (35%)	13 FL 17 Trunc[c]	11.0 (38%)	1

[a] AA, amino acid(s).
[b] ND, not determined.
[c] FL, full-length receptors; Trunc, truncated receptors.

and arrestins that may complicate signaling assay readouts. Thus, the yeast system acts as a reconstitution assay allowing expression of the GPCR of interest and a particular G protein in an isolated environment. The BY1143 strain has been engineered so that activation of the C5aR leads to signaling through the yeast mating pathway resulting in expression of the P_{FUS1}-*HIS3* reporter gene (32). This strain contains a fusion of residues 1–41 of the yeast Gα protein Gpa1, followed by residues 34–354 of the human $G\alpha_{i3}$ subunit. This chimeric G protein allows coupling to both the human C5aR and the endogenous yeast G$\beta\gamma$ (Ste4/Ste18). In addition, the gene encoding the yeast GPCR that normally activates the mating pathway, *STE2*, has been deleted so that the C5aR is the only GPCR present to activate *HIS3* expression. Thus, a functional C5aR allows yeast to grow on histidine-deficient medium. To quantify the relative signaling strength of mutant receptors, the yeast can be grown in the presence of increasing amounts of 3-amino-1,2,4-triazole (3AT), a competitive inhibitor of His3.

The libraries for each region were screened separately in BY1143, and functional receptors were selected on histidine-deficient medium containing 5 mM 3AT. Initial screening demonstrated that both the CT1 and CT2 regions could tolerate many mutations and still function; therefore, these libraries were re-screened, and functional receptors was selected on 100 mM 3AT in an attempt to find the most strongly signaling receptors. An average of 27 functional receptors was selected in each screen, because this has been shown to provide a sufficient number of mutations to determine preserved residues (29, 30, 32, 33). A total of 133 functional receptors were analyzed in this study.

Identification of Preserved Residues—Each region tolerated amino acid substitutions at a different rate, with IC3 allowing the fewest mutations (14%) and CT1 and CT2 allowing the most (35 and 38%, respectively) (Table 1). IC1 and IC2 tolerated amino acid substitution rates of 29 and 28%, respectively. The difference in mutation rates indicates the overall importance of each loop region, because the unselected libraries of receptors all contained similar mutation rates (35–38%).

Specific residues important for signaling are described as "preserved" in our mutagenesis screens if they fit one of three criteria: a position that tolerates no changes; a position that allows only conservative mutations, as identified by a PAM250 matrix log-odds score of 1.0 or greater (41); or a position that undergoes only a single mutation to a non-conserved amino acid. The single non-conserved change is allowed for the possibility that a mutation might be tolerated due to the presence of other compensatory mutations. In addition, we identified positions that retained a hydrophobic amino acid in all mutants. Hydrophobic residues were defined by the partition coefficient of the free amino acid in octanol and water (42). All 133 functional mutants were tested for their ability to signal both in the presence and absence of the C5a ligand; however, none of the receptors were found to be constitutively active. In addition, nearly all mutants (126 of 133) were able to signal better than the wild-type C5aR, indicating selection for a better functioning receptor.

In the IC1 screen, we isolated 28 functional receptors that had an average amino acid substitution rate of 29% (Table 1). Of the 16 amino acids targeted for mutagenesis, only two were preserved: Ile^{70} and Ala^{72} (Fig. 2). These residues are predicted to be part of TM2 based on the rhodopsin crystal structure (3). The hydrophobic nature of Val^{58} was also preserved in this screen; this residue was previously identified as preserved in the screen of TM1 (33). The amino acid changes possible in IC1 due to single nucleotide substitutions have been indicated in the genetic code table, and mutations requiring more than one nucleotide substitution are underlined (Fig. 2). Amino acid changes that occur at a high frequency and that are due to more than one nucleotide substitution can indicate strong selective pressure for certain side-chain properties at a particular position. For example, in IC1, 133 amino acid changes were observed in total. Fourteen of these substitutions occurred as a result of more than one nucleotide substitution within a codon, and seven of these amino acid substitutions were to positively charged amino acids. The molecular basis for the selection is unclear, but the basic amino acids may participate in gain-of-function interactions (*e.g.* between the receptor and G protein that helps facilitate formation of the active state of the receptor) or loss-of-function interactions (*e.g.* removal of a regulatory interaction that keeps the receptor in the basal state, see "Discussion").

The IC2 screen yielded 30 functional receptors with an average amino acid substitution rate of 28% (Table 1). Of the seventeen amino acid positions scanned, six residues remained preserved in the functional C5aRs, and an additional two positions tolerated only hydrophobic amino acids (Fig. 3). Of note, the DRY (DRF) motif, residues Asp^{133}, Arg^{134}, and the hydrophobic nature of position 135, was preserved, as expected based on

	57			60					65					70		72	+C5a					-C5a
IC1	**L**	**V**	**V**	**W**	**V**	**T**	**A**	**F**	**E**	**A**	**K**	**R**	**T**	**I**	**N**	**A**	+	+				0
R3	.	.	.	.	M	.	.	.	.	.	.	.	.	.	.	.	+	+	+	+	+	0
R4	.	*A*	.	*L*	.	S	.	.	.	*V*	.	.	A	.	.	.	+	+	+	+	+	0
R6	F	.	.	*L*	*D*	.	*V*	.	.	T	.	.	.	.	*Y*	.	+	+	+	+	+	0
R9	.	.	.	*L*	.	.	.	.	.	.	.	.	.	.	.	.	+	+	+	+	+	0
R11	*W*	.	.	.	.	*N*	.	.	.	.	.	K	.	.	.	.	+	+	+	+	+	0
R17	.	.	.	.	*D*	.	.	L	D	.	.	.	.	.	.	.	+	+	+	+	+	0
R22	.	.	.	.	*D*	.	T	.	.	.	.	.	.	.	.	.	+	+	+	+	+	0
R23	.	.	.	*L*	.	.	.	*C*	*G*	*V*	.	.	.	.	*T*	S	+	+	+	+	+	0
R24	.	.	.	.	*D*	.	.	Y	.	*V*	.	.	*N*	.	.	.	+	+	+	+	+	0
R25	F	.	.	*C*	.	.	.	L	.	.	.	*T*	.	.	.	.	+	+	+	+	+	0
R26	.	.	I	.	.	S	.	.	.	.	.	K	.	.	.	.	+	+	+	+	+	0
R27	.	.	I	.	*N*	*N*	.	.	.	G	.	.	*N*	.	.	.	+	+	+	+	+	0
R28	.	.	.	*L*	.	S	*Y*	.	.	*K*	.	.	*K*	.	.	.	+	+	+	+	+	0
R29	.	*A*	*F*	.	.	S	.	.	*K*	P	.	.	.	.	*T*	S	+	+	+	+	+	0
R30	.	.	*F*	.	*R*	.	.	*C*	D	.	R	.	*N*	.	H	.	+	+	+	+	+	0
R2	.	.	.	R	I	.	.	.	.	*V*	.	*I*	.	.	.	.	+	+	+	+		0
R5	.	.	.	.	*D*	.	.	*S*	.	*V*	.	*G*	.	.	.	.	+	+	+	+		0
R7	.	.	.	.	*A*	S	.	L	.	G	.	.	*K*	V	S	.	+	+	+	+		0
R10	F	.	.	R	.	.	*R*	.	.	.	.	K	.	.	.	.	+	+	+	+		0
R19	.	.	.	.	*D*	.	.	*C*	.	G	.	.	.	.	.	.	+	+	+	+		0
R21	.	.	.	*L*	.	.	.	.	.	*Q*	*I*	.	S	.	.	.	+	+	+	+		0
R20	.	.	*A*	.	.	.	.	L	.	*R*	.	.	.	.	.	.	+	+	+			0
R1	*S*	.	*G*	.	.	.	.	.	.	*K*	*P*	.	*P*	V	.	.	+	+				0
R14	.	.	*A*	*L*	*D*	.	.	.	*A*	P	R	.	*P*	V	.	.	+	+				0
R16	.	.	L	.	.	.	.	*V*	Q	*N*	.	.	.	.	.	S	+	+				0
R12	.	.	*G*	.	.	.	*V*	I	.	.	.	K	*I*	V	*T*	S	+					0
R13	.	.	.	R	.	.	.	*W*	.	*V*	N	*S*	.	.	.	.	+					0
R15	F	.	*F*	*C*	.	.	.	*V*	.	.	R	*I*	.	.	.	.	+					0
Genetic Code	*S*	*D*	*D*	@	*D*	*I*	*D*	*C*	@	*D*	@	@	*I*	*N*	*I*	S						
	@	*F*	*F*	*C*	*F*	*N*	*V*	*S*	*G*	*V*	*T*	*C*	*N*	*S*	*Y*	P						
	W	*G*	*G*	*G*	*G*	*P*	G	*V*	*K*	G	*E*	*G*	*P*	*T*	*T*	T						
	F	*A*	*A*	*L*	*A*	A	P	Y	*V*	P	*I*	*I*	A	V	D							
		I	I	*S*	I	S	S	L	*A*	S	Q	*T*	S	L	H							
		L	L	R	L		T	I	Q	T	R	*S*		M	K							
									D		N	K		F	S							
Preserved Hydrophobic														X		X						
		X												X								
IC1	**L**	**V**	**V**	**W**	**V**	**T**	**A**	**F**	**E**	**A**	**K**	**R**	**T**	**I**	**N**	**A**						
	57			60					65					70		72						

FIGURE 2. **Analysis of the first intracellular loop of the C5aR.** The wild-type sequence of the region targeted by mutagenesis in IC1 is given (*top* and *bottom* in *bold*) with the residue numbers marked. The amino acid sequences of the functional mutant receptors obtained (designated by "*R*" and a number, *left*) are indicated (*dot*, unchanged amino acid compared with wild-type). *Italicized letters* denote amino acid changes that are not conserved with respect to the wild-type C5aR sequence (see text). Signaling strength of each receptor is shown in the presence (+*C5a*) and in the absence (−*C5a*) of ligand: +++++, growth on 50 mM 3AT; ++++, growth on 20 mM 3AT; +++, growth on 10 mM 3AT; ++, growth on 5 mM 3AT; +, growth on 1 mM 3AT; 0, no growth on 1 mM 3AT. Residues that are preserved or have hydrophobicity preserved are marked (indicated by *X* in *boxed rows*; see text for definitions). "*Genetic code*" refers to the amino acids available via a single nucleotide substitution. Mutations requiring more than one nucleotide substitution are *underlined*. @, indicates a stop codon.

the essential nature of this motif in G protein activation by rhodopsin-like GPCRs (8–10). A striking number of mutant receptors (23 of 30) contained an amino acid substitution at position 145 with a strong propensity for replacement of the glutamine with an amino acid containing a positively charged side chain (19 of the 23). This could be due to selection of better functioning receptors, because all the IC2 mutants signal more strongly than the wild-type C5aR. Again, this may reflect introduction of a positive interaction within the receptor or between the receptor and G protein that helps facilitate formation of the active state of the receptor, or removal of a negative regulatory interaction that keeps the receptor in the basal state.

Eighteen functional IC3 mutant receptors were selected with an average amino acid substitution rate of only 14.2% (Table 1).

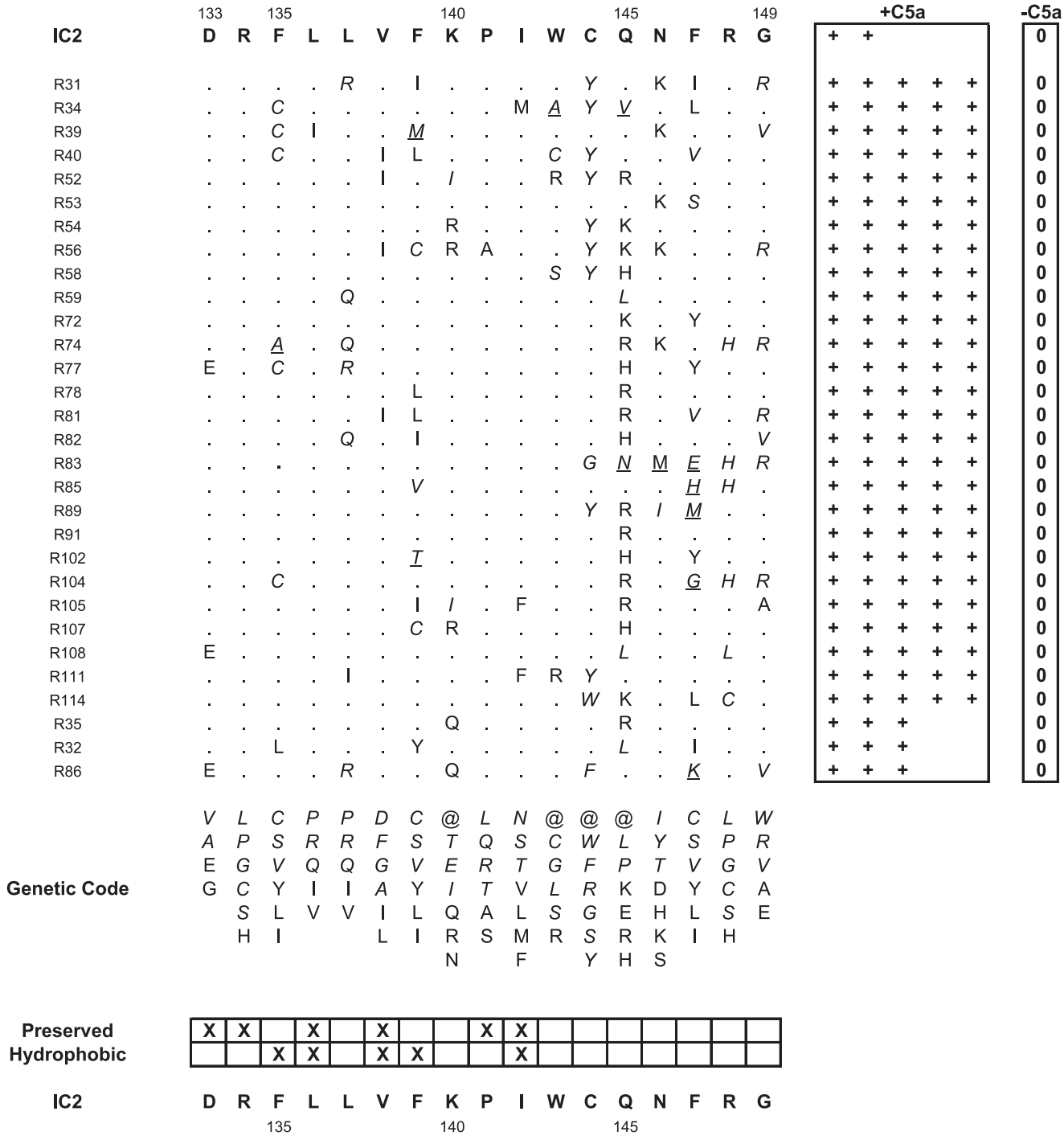

FIGURE 3. **Analysis of the second intracellular loop of the C5aR.** The wild-type sequence of the region targeted by mutagenesis in IC2 is given (*top* and *bottom* in *bold*) with the residue numbers marked. The amino acid sequences of the functional mutant receptors obtained (designated by "*R*" and a number, *left*) are also indicated and annotated as in Fig. 2.

Of the 21 amino acid positions targeted in this screen, 11 were preserved (Fig. 4). In addition to the 11 preserved residues, 3 other positions preserved hydrophobicity. Thus, only 7 residues of 21 in this short stretch of sequence allowed a change in the nature of the amino acid, making this region the least susceptible to mutation of any region of the C5aR, including the TM segments (32, 33), and the extracellular loops (29, 30). This demonstrates an essential role of IC3 in G protein binding, activation, and/or receptor folding. Of note, Val^{244} demonstrated a strong propensity to mutate to a serine, even though this requires two nucleotide substitutions to occur.

The highly preserved nature of the IC3 region is in stark contrast to the results obtained for the carboxyl-terminal regions. 27 functional receptors with an average amino acid substitution rate of 35% were selected from the CT1 library (Table 1). 14 were full-length receptors, and 13 were truncated (Fig. 5). Of the 14 residues tested, only one position, Arg^{310}, was preserved among the full-length receptors. An additional three

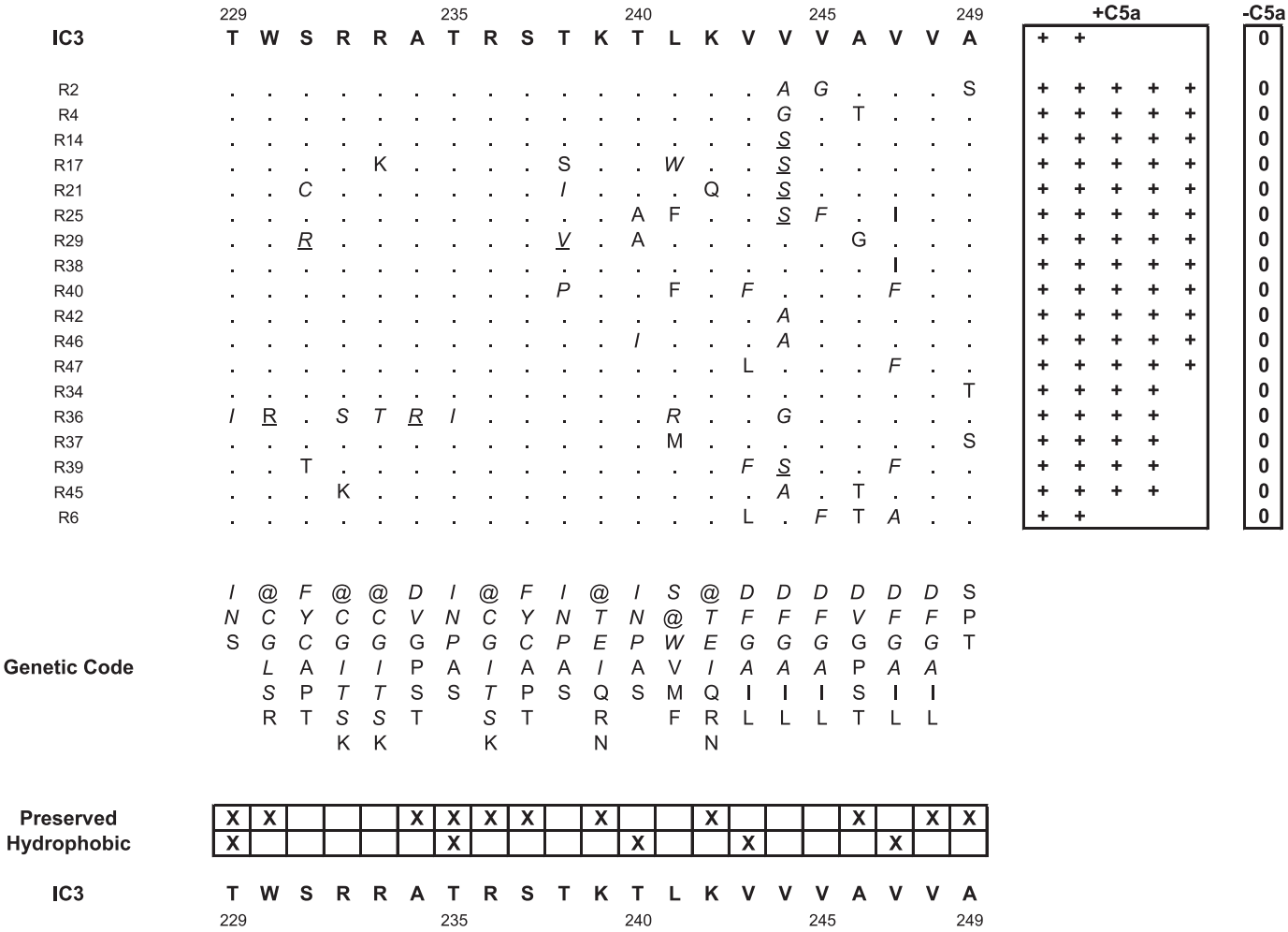

FIGURE 4. **Analysis of the third intracellular loop of the C5aR.** The wild-type sequence of the region targeted by mutagenesis in IC3 is given (*top* and *bottom* in *bold*) with the residue numbers marked. The amino acid sequences of the functional mutant receptors obtained (designated by "*R*" and a number, *left*) are also indicated and annotated as in Fig. 2.

residues preserved hydrophobicity in the full-length receptors (Leu^{310}, Leu^{315}, and Leu^{318}). With the small number of full-length receptors in the CT1 data set, the significance of preserved residues is less clear than in the case of the intracellular loops. Among the truncated receptors a stop codon was observed as early as position 311. This indicates that the C-terminal 40 amino acids are not essential for G protein activation in the yeast system.

For the CT2 screen, 30 functional receptors were selected, 17 of which were truncated receptors (Table 1). An average amino acid substitution rate of 38% was observed in the full-length receptors. Many types of mutations were tolerated at numerous positions within any given receptor (Fig. 6). Of the 29 residues tested, only one position (Val^{328}) was preserved among the full-length receptors. Even though residue Asn^{321} mutated solely to a lysine, it was not considered preserved, because, due to the design of the library, only two of the three nucleotides in its codon were allowed to mutate. No other residues preserved hydrophobicity in the full-length receptors. Unlike in the intracellular loops, the patterns of amino acid substitutions did not suggest a strong selection for a particular amino acid or type of side chain at any one position. Taken together, the number of preserved residues in each region targeted allows us to rank the relative importance of each intracellular loop in C5aR signaling with IC3 being the most important with 11 of 21 residues preserved, followed by IC2 with 6 of 17 residues preserved, IC1 with 2, and finally CT1 and CT2 with 1 preserved residue each.

The majority of the receptors isolated in the five screens signaled stronger than the wild-type C5aR (126 of 133). To test whether signaling strength correlates with receptor expression level, we performed Western blot analyses on mutant receptors that signaled in the presence of high concentrations of 3AT or at levels comparable to the wild-type C5aR (Fig. 7*A*). In general, the mutated C5aRs obtained in the selection did express at higher levels than the wild-type C5aR, but there was no clear correlation between expression and signaling levels. For example, weak signalers such as IC1 R13 and R14 are expressed at relatively high levels, whereas strong signalers such as IC2 R89 and CT2 R9 are expressed at low levels. In addition there are weak signalers expressed at low levels, like IC1 R1 and strong signalers with high levels of expression such as IC3 R2. This analysis detects steady-state levels of the expressed receptors. Therefore, it is possible that strong signaling receptors could be desensitized and therefore appear to be expressed at low levels. We cannot rule out this possibility. However, we do not see any evidence for C5aR internalization in response to ligand activa-

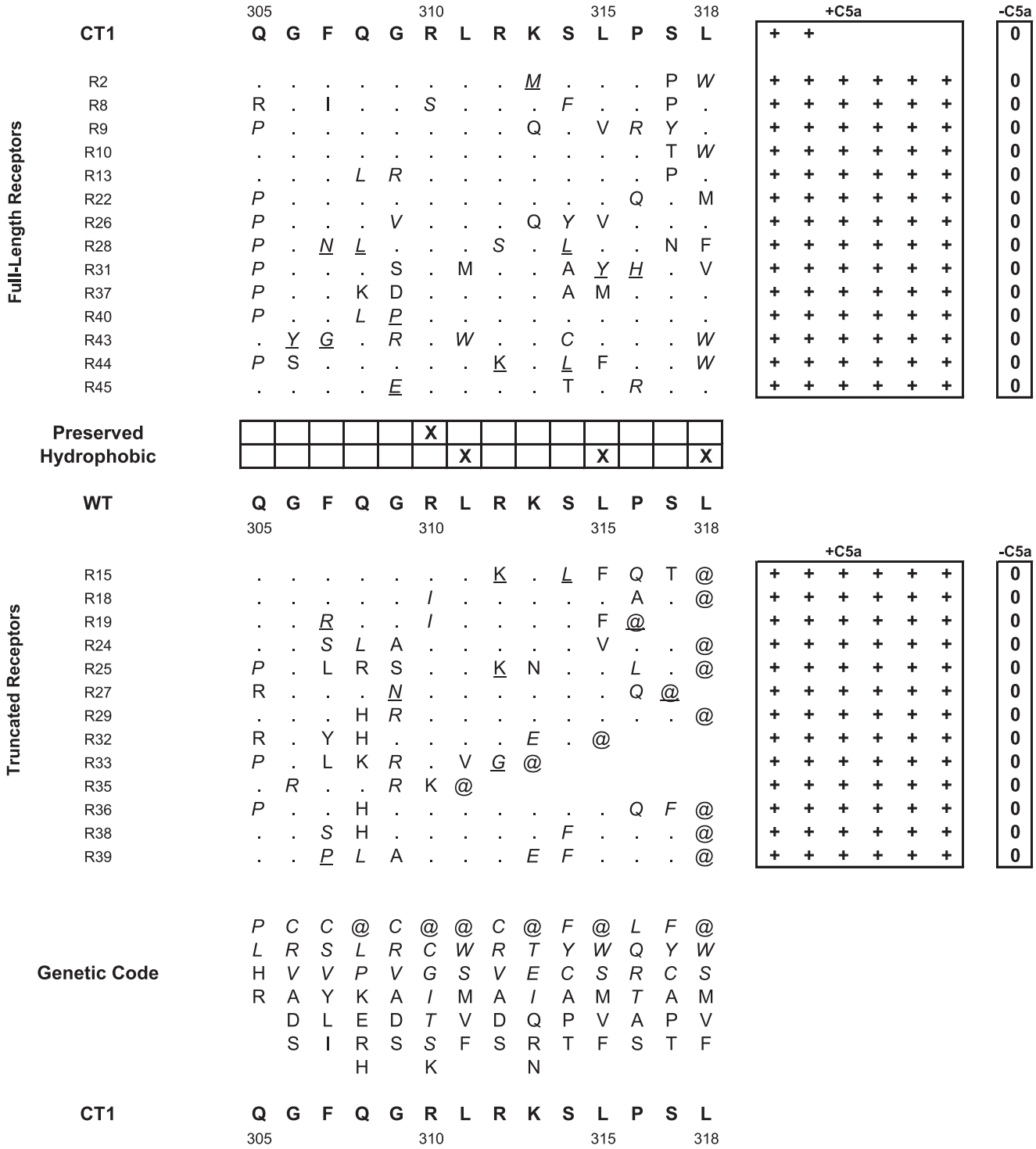

FIGURE 5. **Analysis of the first half of the C terminus of the C5aR.** The wild-type sequence of the region targeted by mutagenesis in CT1 is given (*top* and *bottom* in *bold*) with the residue numbers marked. The amino acid sequences of the functional mutant receptors obtained (designated by "*R*" and a number, *left*) are also indicated, with the full-length receptors on the *top* and the truncated receptors on the *bottom*. ++++++, growth on 100 mM 3AT. The sequences are annotated as in Fig. 2.

tion (data not shown). The mechanisms in yeast that mediate pheromone receptor (Ste2) desensitization (phosphorylation of the Ste2 carboxyl terminus, ubiquitination, and physical association of Ste2 and SstII (the yeast RGS protein)) (43–45) most likely do not operate on the C5aR expressed in yeast.

Signaling of the C5aR in yeast leads to cell growth through the action of free G$\beta\gamma$ that has been released from Gα upon GTP binding (46). Thus, a mutant receptor may permit cell growth by binding and sequestering Gα without actually catalyzing GTP exchange, leaving G$\beta\gamma$ free to signal. To evaluate this possibility, we expressed the wild-type C5aR or various mutants from the screens in the BY1143 strain in the presence and absence of the mammalian GTPase-activating protein, RGS4 (Table 2). Signaling of the wild-type C5aR and all mutants

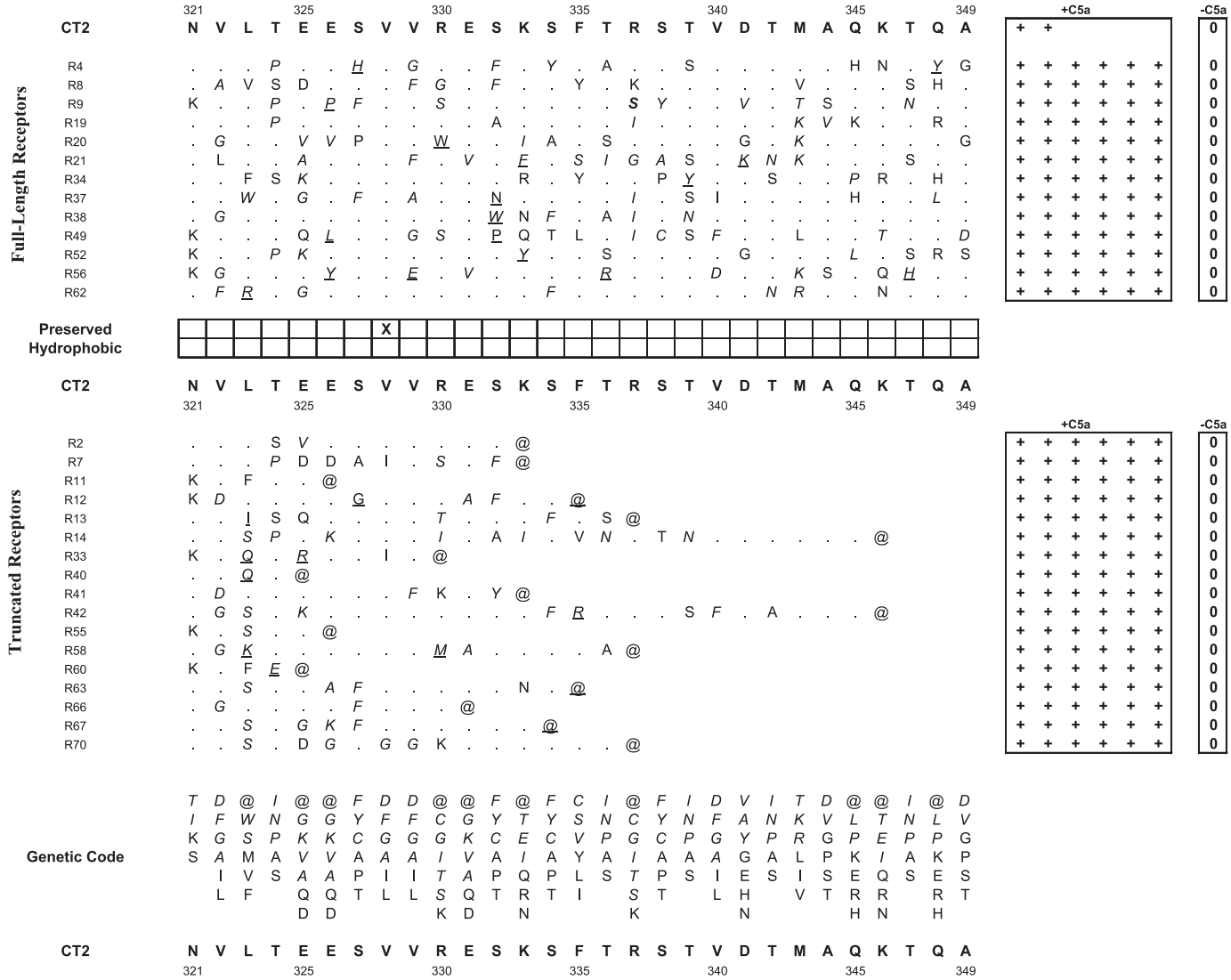

FIGURE 6. **Analysis of the second half of the C terminus of the C5aR.** The wild-type sequence of the region targeted by mutagenesis in CT2 is given (*top* and *bottom* in *bold*) with the residue numbers marked. The amino acid sequences of the functional mutant receptors obtained (designated by "*R*" and a number, *left*) are also indicated, with the full-length receptors on the *top* and the truncated receptors on the bottom. ++++++, growth on 100 mM 3AT. The sequences are annotated as in Fig. 2.

tested was sensitive to RGS4 expression indicating that these receptors likely catalyze Gα-GDP turnover.

Characterization of Preserved Residues—To validate the findings of the saturation mutagenesis studies, preserved residues were then tested by site-directed mutagenesis. Each preserved residue was mutated individually to alanine or, if it was already an alanine, to a larger hydrophobic residue. Additionally, each position that preserved hydrophobicity in the screens was tested by mutating the hydrophobic residue to asparagine. Asparagine was chosen because it is a polar residue that does not contain a fully charged side chain. Each point mutant was then assayed for signaling in the BY1143 strain (Table 3).

IC3 had the greatest number of preserved residues out of all the screened regions. Eight of these eleven residues, when mutated, yielded receptors with little to no signaling (Trp^{230}, Ala^{234}, Thr^{235}, Arg^{236}, Ser^{237}, Lys^{239}, Val^{248}, and Ala^{249}). In IC2, point mutants D133A and R134A of IC2 abolished signaling of the receptor and the hydrophobic nature of position 135 was also important in that the F135N mutation impairs signaling of the receptor compared with wild-type C5aR. Also, Pro^{141} was important in C5aR function as seen by the impaired signaling of the P141A mutant. A recent study demonstrated that this highly conserved proline residue in GPCRs serves as a β-arrestin binding determinant (47). The fact that this proline residue was also preserved in our yeast screens, despite the fact that yeast does not contain a β-arrestin homolog, indicates that this residue must serve another important function in addition to allowing β-arrestin binding. In fact, this residue was also shown to be necessary for the 5HT2c receptor to couple to Gα_q (47). The hydrophobic nature of Ile^{142} was required for signaling, as an I142N mutation abolished signaling. A hydrophobic residue in the center of IC2 corresponding to position 142 of the C5aR has also been shown to be essential for signaling in several other receptors (2, 48–50). A hydrophobic residue at position 311 of CT1 was also necessary for C5aR signaling.

Not all preserved residues resulted in a loss of function when mutated (Table 3). It is possible that other neighboring residues in the context of the wild-type receptor can compensate for the

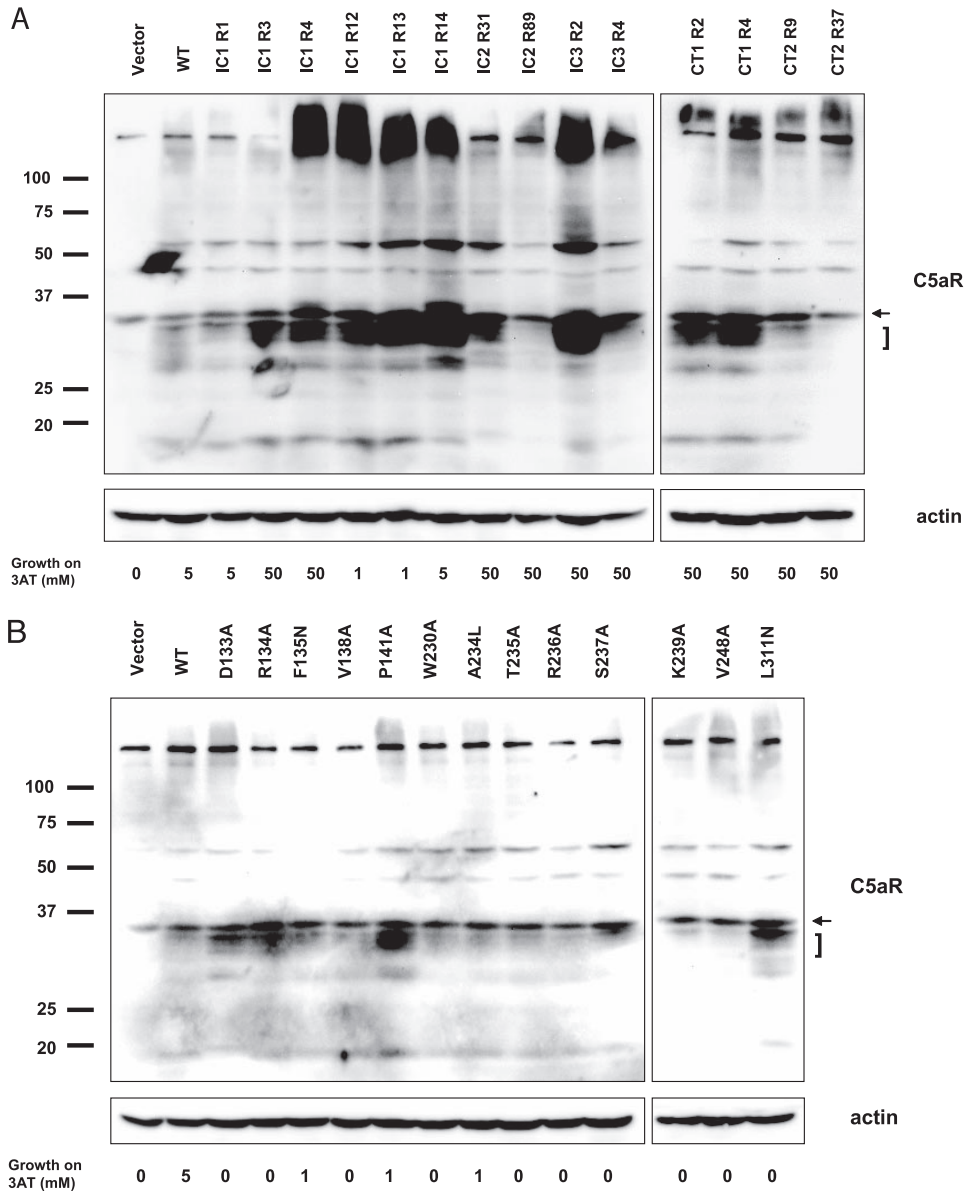

FIGURE 7. **Expression levels of mutant receptors.** *A*, RSM mutants from the screens showing varying levels of signaling and *B*, single point mutants that showed impaired signaling by the growth assay (Table 3) were assayed for receptor expression levels. BY1142 carrying an empty vector, a plasmid expressing wild-type C5aR (*WT*), or individual mutants were lysed and separated by SDS-PAGE. Western blots were probed with an anti-C5aR antibody, stripped, and reprobed with an anti-β-actin antibody as a loading control. A nonspecific band recognized by the anti-C5aR antibody is indicated by an *arrow*. Monomeric C5aR migrates as a triplet (30–35 kDa) directly below the nonspecific band and is indicated by a *bracket*. The triplet is presumably due to oligosaccharide addition and processing. Proteolytic fragments and oligomers of the receptor migrate faster and slower than the monomer, respectively. The signaling strengths of each receptor indicated below the Western blots are reported as the maximal amount of 3AT (mM) that permits receptor-dependent growth of the yeast.

signaling is not simply due to decreased receptor expression. Blots probed with an anti-β-actin antibody demonstrated equal loading. In addition, YFP tags were added to all non-functional mutant receptors to assess localization by fluorescent microscopy (supplemental Fig. S1). All mutants demonstrated membrane staining similar to the wild-type receptor. YFP-tagged mutants were also analyzed by Western blot using an anti-GFP antibody (supplemental Fig. S2). All point mutants are expressed at levels similar to, if not greater than the wild-type C5aR.

The point mutants were also expressed in BY1173, which contains a P_{FUS1}-β-galactosidase reporter gene providing a growth-independent assay of signaling. Use of the C5aR hexapeptide agonist W5Cha allows dose-response curves to be generated, because, unlike C5a, W5Cha can cross the yeast cell wall. Wild-type C5aR activates the P_{FUS1}-β-galactosidase reporter gene in a dose-dependent manner in response to W5Cha (Fig. 8, *A* and *B*). The dose-response curves of all mutants tested show decreased potency and efficacy. Even the most active mutant, W230A, displays only 50% maximal activity compared with the wild-type receptor. Thus, all of these residues are important, to varying degrees, for wild-type level activation of the C5aR in response to both C5a and W5Cha.

To distinguish between point mutations that affect the overall folding of the receptor *versus* receptor activation, we also expressed the single point mutant receptors in HEK293 cells. In mammalian cells, improperly folded receptors are retained in the endoplasmic reticulum (ER). This can readily be determined by monitoring the processing of the *N*-linked oligosaccharides on the receptor. Lysates were subjected to Endo-H_f treatment (Fig. 9*A*). Endo-H_f cannot cleave complex *N*-linked oligosaccharides that are formed in the Golgi but can remove the high mannose sugars added in the ER. Endo-H_f resistance indicates that the receptor exited the ER, passed through the Golgi, and likely made it to the cell surface. Only D133A was completely Endo-H_f-sensitive, indicating that this mutant fails to exit the ER. All other mutants tested demon-

role these amino acids play in receptor function, and only in the presence of other mutations do these residues play significant roles. In fact the power of the system lies in the ability to determine residues important for function that would otherwise be missed in a traditional alanine scanning experiment.

Point mutants that demonstrated reduced signaling compared with the wild-type receptor, or no signaling at all, were further characterized by Western blot analysis (Fig. 7*B*). All mutant receptors were expressed at levels comparable to, if not greater than the wild-type C5aR, indicating that their impaired

strate Endo-H_f-resistant receptor levels comparable to the wild-type C5aR, indicating proper localization of these receptors.

In addition, we characterized the signaling of these mutants in mammalian cells. The receptors were co-transfected with the promiscuous human $G\alpha_{16}$ subunit, and inositol 1,4,5-triphosphate (IP_3) accumulation was determined after treatment with 0.1 μM W5Cha or 1 μM W5Cha (Fig. 9*B*). The wild-type C5aR shows robust IP_3 accumulation upon stimulation with both concentrations of W5Cha. D133A shows no signaling, consistent with its inability to reach the cell surface. With the exception of W230A, all of the mutants demonstrated impaired signaling compared with the wild-type C5aR ($p < 0.05$ at 0.1 μM W5Cha). W230A is the most active of the mutants, and K239A is severely impaired, which was also the case in the yeast β-galactosidase assay. Some receptors such as R134A and V138A show wild-type level signaling when treated with 1 μM W5Cha, whereas others like R236A and K239A are still impaired. In general, these results correlate with the receptor phenotypes in yeast; however, the effect of each mutation is less severe in the context of the mammalian system. This is not surprising given the fact that single-cysteine substitutions in the intracellular loops and carboxyl terminus of bovine rhodopsin rarely led to completely non-functional receptors (13–16). The differences between signaling levels of the C5aR mutants in yeast and mammalian cells may reflect that receptor-G protein interactions are more robust in their native environment.

Modeling of the C5aR Intracellular Loops—The random saturation mutagenesis identified positions that were preserved, *i.e.* did not tolerate substitutions. Mapping these residues onto a three-dimensional structure for the intracellular loops would be very helpful in understanding their functional significance. However, the intracellular loops in the C5aR are similar but not identical to those in rhodopsin, which is the only available three-dimensional template for GPCRs. Also, the intracellular loops are flexible; for example, the rhodopsin IC3 loop possesses distinctly different conformations in different experimental x-ray structures (3–7). Accordingly, the mapping should account for a variety of loop conformations. Using methodologies we developed to model the loops of rhodopsin in the active and inactive states (36) (see "Experimental Procedures" for details), we performed molecular modeling to determine potential conformations of the intracellular loops in the C5aR. The modeling predicted 16 energetically reasonable combinations of conformations of the intracellular loops, each differing from the others by the accepted r.m.s.d. cut-off value of 2 Å (Fig. 10*a*). In fact, the combinations differed almost exclusively in their predictions for IC2, ranging from an "open" to a "closed" structure (compare different *magenta-shaded ribbons* in Fig. 10*a*), whereas IC3 retained basically the same structure in all predicted models. This was in contrast with the results obtained earlier for rhodopsin (36), where the modeling procedure for the dark-adapted state of the TM bundle revealed 13 combinations of possible conformations for the intracellular loops that differed mostly in the structures of the more flexible IC3 (in accordance with experimental structural data mentioned above), rather than in the conformation of IC2. One possible reason for this is that IC3 of rhodopsin is longer by nine residues and IC2 shorter by one residue than their respective counterparts in the C5aR. Low energy conformations of the IC2 loop were stabilized mostly by the residue-residue interactions

TABLE 2

RGS4 effect on receptor signaling

The wild-type C5aR and various mutant receptors from the screens were transformed into BY1143 in the presence (+RGS4) or absence (−RGS4) of the GTPase-activating protein, RGS4. Signaling was assayed on histidine-deficient medium with varying concentrations of 3AT for three independent transformants: +++++, growth on 50 mM 3AT; ++++, growth on 20 mM 3AT; +++, growth on 10 mM 3AT; ++, growth on 5 mM 3AT; +, growth on 1 mM 3AT; 0, no growth on 1 mM 3AT. RGS4, GTPase activating protein; WT, wild-type C5aR.

Receptor	−RGS4	+RGS4
WT	++	0
IC1 R4	+++++	0
IC1 R14	++	0
IC2 R31	+++++	0
IC2 R89	+++++	0
IC3 R2	+++++	0
IC3 R4	+++++	0
CT1 R2	+++++	0
CT1 R8	+++++	0
CT2 R2	+++++	0
CT2 R9	+++++	0
CT2 R14	+++++	0
CT2 R19	+++++	0
CT2 R37	+++++	0
CT2 R56	+++++	0
CT2 R66	+++++	0
CT2 R70	+++++	0

TABLE 3

Signaling of individual point mutants

The mutants indicated were transformed into BY1143 expressing the C5a ligand (+C5a). Signaling was assayed on histidine-deficient medium with varying concentrations of 3AT for three independent transformants: +++++, growth on 50 mM 3AT; ++++, growth on 20 mM 3AT; +++, growth on 10 mM 3AT; ++, growth on 5 mM 3AT; +, growth on 1 mM 3AT; 0, no growth on 1 mM 3AT; WT, wild-type C5aR.

IC1		IC2		IC3		CT1		CT2	
Mutant	+C5a	Mutant	+C5a	Mutant	+C5a	Mutant	+C5a	Mutant	+C5a
WT	++	WT	++	WT	++	WT	++	WT	++
I70A	++++	D133A	0	T229A	+++++	G306V	++	V328Q	++++
A72V	++	R134A	0	W230A	0	R310A	++		
		F135N	+	A234L	+	L311N	0		
		L136A	++	T235A	0	L315N	+++++		
		V138A	0	R236A	0	L318N	+++++		
		F139N	+++	S237A	0				
		P141A	+	K239A	0				
		I142A	++	K242A	++				
		I142N	0	V243N	+++				
				A246V	++++				
				V247N	+++++				
				V248A	0				
				A249V	+				

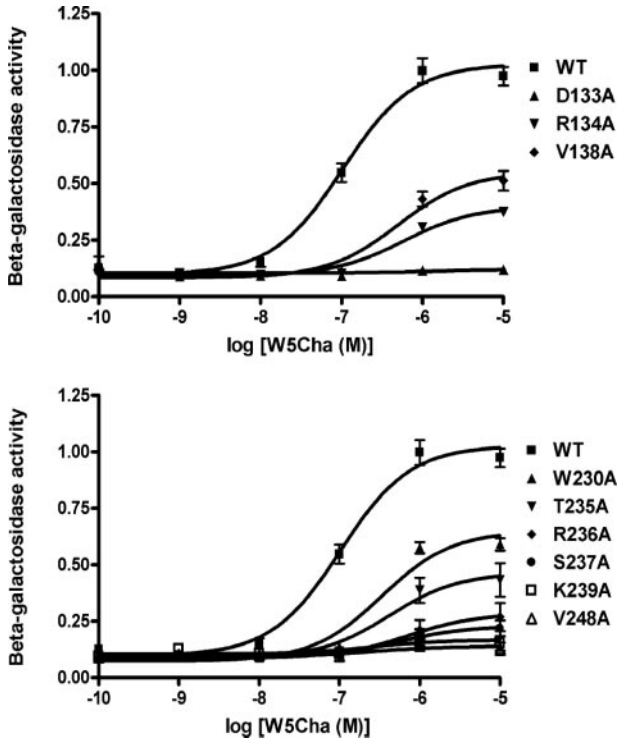

FIGURE 8. **Dose-response curves of the single point mutants.** Single point mutants in IC2 (*A*) or IC3 (*B*) that did not show signaling by the growth assay (Table 3) were tested for activation of the P_{FUS1}-β-galactosidase reporter gene. BY1173 transformed with either wild-type or mutant receptors was treated with increasing concentrations of the hexapeptide agonist W5Cha and assayed for β-galactosidase activity. The mean of each experiment done with three independent transformants, each in triplicate is shown, ± S.D. All values are normalized to the E_{max} of the wild-type receptor.

within the IC2 loop, especially in the open conformations. In some closed structures, interactions between IC2 and the other intracellular loops were observed.

When the residues elucidated by our screens are mapped on the three-dimensional structure of the C5aR that corresponds to one of the open conformations of IC2, an interesting image emerges (Fig. 10*b*). All of these residues map to one half of the intracellular face of the C5aR structure. They are found in the TM3 helix close to the IC2 loop as well as the relatively rigid IC3 loop and its adjacent TM6 helix. Most of the preserved residues identified belong, in fact, to TM helices, as they were defined in our modeling procedure (see "Experimental Procedures"), including Asp^{133}, Arg^{134}, and Val^{138} (TM3), and Arg^{236}, Ser^{237}, Lys^{239}, and Val^{248} (TM6). The same is true for the "required hydrophobic" residue Phe^{135} (TM3) and the residue Val^{244} (TM6). Obviously, spatial positions of these TM helix residues remain close regardless of the conformations of the loops. Also, because conformational flexibility of IC3 is limited by rather similar energetically feasible structures (see Fig. 10*a*), spatial positions of residues Trp^{230} and Thr^{235} are also close to each other and do not depend on the specific conformation of IC2.

DISCUSSION

In this study we have performed a comprehensive structure-function analysis of the C5aR to identify all residues on the intracellular surface required for signaling through "humanized" G proteins in yeast. Although other studies have focused on a single loop of a specific receptor (25–28), this is the first complete functional map of the intracellular face of any GPCR generated by random saturation mutagenesis. These data in combination with our previous studies on the TM and extracellular loop regions gives a comprehensive view of residues most important for the structure and function of the C5aR (29–33).

Comparison of our data set to comprehensive studies of two other well characterized receptors, bovine rhodopsin (*Rhod*) and the m5 muscarinic acetylcholine receptor (*m5R*), reveals many similar required residues (Fig. 11). An RSM experiment was performed by the Brann laboratory on the IC2 region of the m5R where receptors were selected for coupling to $G\alpha_q$ in mammalian cells (27). Comparison of our IC2 RSM data and that of the Brann group reveals striking similarities (Fig. 11). All six of the preserved IC2 residues identified in our screen were also preserved in the m5R screens. These include the DRY/DRF motif and the residues that correspond to the C5aR positions Val^{138}, Pro^{141}, and Ile^{142}. Only two preserved positions were found in the m5R but not in the C5aR. Despite the fact that the C5aR and the m5R couple to different G proteins and that these screens were performed in yeast and mammalian systems, respectively, there is significant overlap in the preserved residues. This indicates that these residues and IC2 as a whole likely play a role in G protein activation through a mechanism common to both $G\alpha_i$ and $G\alpha_q$ G proteins. There was also partial overlap between residues that did not tolerate mutation in rhodopsin IC2 studies (8, 17, 51, 52) and in our C5aR screen (Fig. 11). These include the DRF/ERY motif and the position that corresponds to Val^{138} in the C5aR.

RSM screens of the IC3 region of the m5R (25, 26) and mutagenesis of IC3 in rhodopsin (8, 14, 17, 52, 53) have also been performed. However, the length of IC3 is quite variable (~230, 21, and 13 amino acids for the m5R, rhodopsin, and C5aR, respectively) (Fig. 11). It is therefore more difficult than for IC2 to align the loops and compare individual residues. Relative to other rhodopsin family members, C5aR possesses a small IC3 loop. The significance of this for receptor activity is unclear. Nevertheless, the preserved residues cluster near the end of TM5 and the beginning of IC3, as well as the end of IC3 and the beginning of TM6, in all three receptors. Furthermore, the dispensability of the intervening sequences is underscored by the fact that deletion of the central portion of large IC3 loops does not impair signaling (reviewed in Ref. 54).

The carboxyl-terminal tails of these three receptors are even more divergent than the IC3 loops. Some essential residues have been identified in the tails of rhodopsin (17) and the C5aR (55) (Fig. 11). However, no essential residues were found in our screen and no essential residues in the m5R tail have, to our knowledge, been reported to date. One surprising finding in our carboxyl-terminal tail screens was the abundance of truncated, yet functional receptors. Previous studies in mammalian cells showed that mutation of Gln^{305} to a stop codon prevented cell surface expression of the C5aR (55), which we also demonstrate in the accompanying paper (Matsumoto, *et al.* (82)). The carboxyl terminus has also been shown to be involved in folding and trafficking of other GPCRs (56–63). This folding requirement has obviated the ability to assay severely truncated receptors for G protein activation. Thus, use of the yeast system

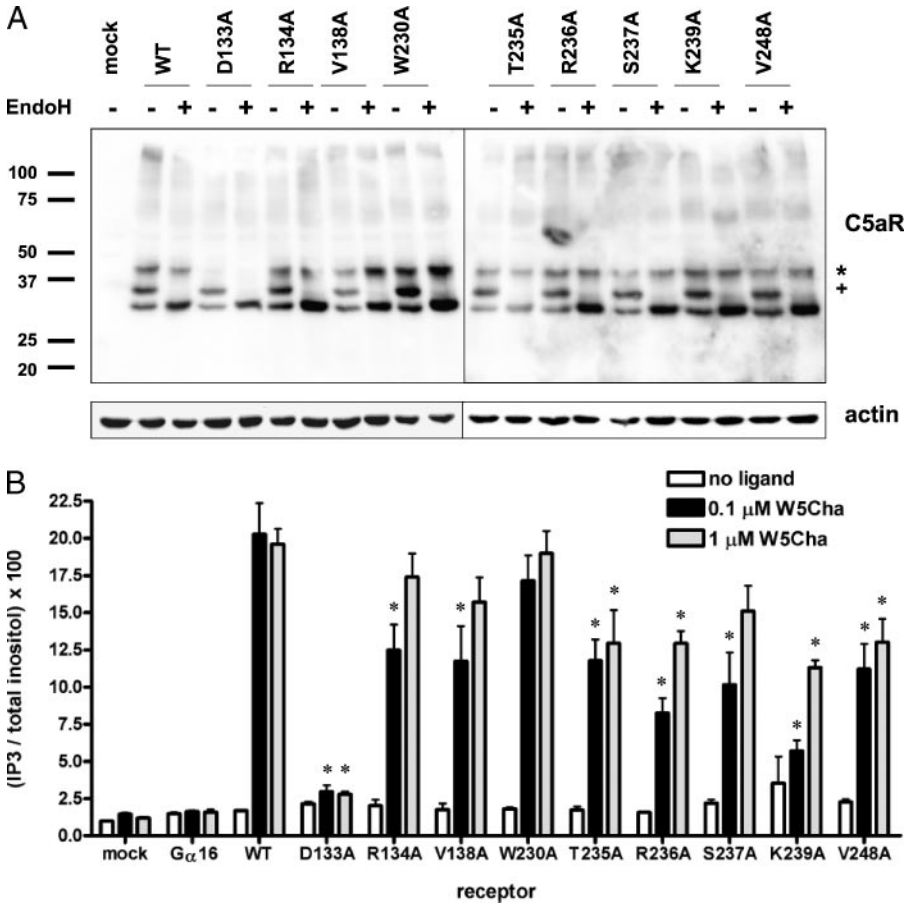

FIGURE 9. **Single point mutants in mammalian cells.** *A*, lysates of HEK293 cells transiently transfected with wild-type C5aR (*WT*) or single point mutants were treated with (+) or without (−) Endo-H_f and analyzed by immunoblotting for C5aR. Blots were then stripped and reprobed with an anti-β-actin antibody as a loading control. Endo-H_f-resistant receptors containing complex *N*-linked oligosaccharides (*) and Endo-H_f-sensitive high mannose oligosaccharides (+) are shown. *B*, HEK293 cells transiently transfected with $G\alpha_{16}$, $G\alpha_{16}$ plus wild-type C5aR (*WT*), or $G\alpha_{16}$ plus single point mutants were treated with no ligand, 0.1 μM, or 1 μM W5Cha and assayed for IP_3 accumulation. Values are normalized to the mock transfection without ligand. Each *bar* represents the mean of three independent trials, ± S.D. One-way analysis of variance tests were performed where mutants were compared with the wild-type value of the corresponding ligand concentration. $p < 0.05$ is indicated by an *asterisk*.

allowed us to uncover the dispensability of the tail of the C5aR in G protein activation, an observation that could not be made in mammalian cell studies due to the essential role of the tail in trafficking. The C5aR lacks a cysteine in the carboxyl terminus that is palmitoylated in rhodopsin. This modification results in a fourth intracellular loop structure in many of the rhodopsin family members. It is unclear if these receptors might display a greater dependence on the presence of the carboxyl terminus. In addition, whereas our results demonstrate that the carboxyl terminus of the C5aR is dispensable in the context of signaling in the yeast system, the tail plays important roles in other aspects of C5aR signaling such as desensitization, internalization, and interaction with accessory proteins (64–68). In addition, the carboxyl terminus likely does participate in G protein activation either by determining specificity or regulating the rate of G protein activation (accompanying paper: Matsumoto, *et al.* (82) and Ref. 69). These elements of tuning the signaling properties are likely very important for receptor biology in complex processes like neutrophil chemotaxis.

Nearly all mutants identified in our screens (126 of 133) were able to signal better than the wild-type C5aR. In some instances there was selection for one or more particular amino acids. These include the high frequency of positively charged residues inserted into IC1 due to more than one nucleotide substitution (Fig. 2), IC2 receptors containing a mutation of Gln^{145} to a positively charged residue (Fig. 3), and IC3 receptors containing a V244S substitution (Fig. 4). This could reflect either addition of a positive interaction within the receptor or between the receptor and G protein that helps facilitate formation of the active state of the receptor or removal of a negative regulatory interaction that keeps the receptor in the basal state.

There are three major classes of positive interactions that could lead to a more strongly signaling receptor. First, introduction of positively charged or polar residues could favor interaction with the negatively charged phospholipid head groups of the plasma membrane (70) thereby stabilizing the receptor or facilitating formation of the active state.

Second, creating a stronger interaction of the receptor with the G protein could also increase signaling. A particular strength of performing RSM screens in the yeast system lies in the ability to detect possible "evolution" of the receptor toward a better interaction with the chimeric G protein. The Gα chimera, consisting of residues 1–41 of yeast Gpa1 followed by residues 34–354 of human $G\alpha_{i3}$, was used to allow coupling to the yeast Gβγ and the downstream components of the mating pathway. The amino terminus of $G\alpha_{i3}$ (residues 1–33) contains nine residues that have negatively charged or polar side chains (Asp, Glu, Asn, and Gln). In comparison, the amino terminus of Gpa1 (residues 1–41) contains 16 negatively charged or polar residues, thus potentially creating a much more negative electrostatic potential on the amino terminus of the yeast chimera than human $G\alpha_{i3}$. IC1 functional mutants revealed an abundance of positively charged residues that required more than one nucleotide substitution, suggesting that IC1 could make contact with the amino terminus of the Gα subunit. Interestingly, one possible model of bovine rhodopsin docked to the transducin heterotrimer demonstrates an ionic interaction between Lys^{67} of the IC1 loop of rhodopsin and Glu^{14} of the amino terminus of $G\alpha_t$ (71). Lys^{67} of rhodopsin corresponds to Ala^{66} of the C5aR, the position that mutated most frequently to a positively charged residue through more than one nucleotide substitution in our IC1 screen (Fig. 2). In addition, several stud-

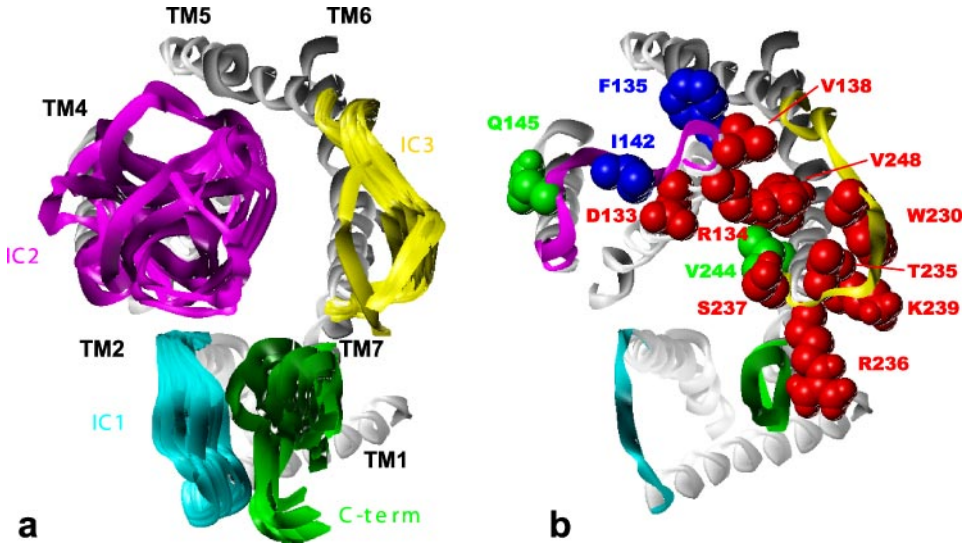

FIGURE 10. **Model of the activation face.** *a*, sketches of energetically feasible options for spatial positions of the intracellular loops in the C5aR. Backbone conformations of TM helices are shown as *white shaded ribbons* and are numbered; different backbone conformations of the intracellular loops and carboxyl terminus (*C-term*) (fragment 300–310) are shown as *colored ribbons* with IC1 in *cyan*, IC2 in *magenta*, IC3 in *yellow*, and the carboxyl terminus in *green*. The view is from the intracellular side of the membrane. *b*, side chains of several important residues are shown as space-filled models for a loop conformation with an open position of IC2. The preserved residues are shown in *red*, the required hydrophobic residues Phe[135] and Ile[142] in *blue*, and *green* denotes residues that mutated at high rates to specific amino acids (Q145R, K, H, and V244S). For simplicity, only the preserved residues that did not tolerate point mutations are displayed.

IC1

C5aR ^{55}NALVVWVTAFEAK-RTINAIWFLNL^{78}
Rhod ^{55}NFLTLYVTVQ**HKKLRT**PLNYILLNL^{79}
m5R ^{48}NVLVMISFKVNSQLKTVNNYYLLSL^{72}

IC2

C5aR ^{133}*D*RFLLVFKPIWCQNFRGAGLAWIA*C*AVAW^{161}
Rhod ^{134}ERYVVV**CKPMSNFRFG-E**NHAIMGVAFTW^{161}
m5R ^{127}DRYFSITRPLTYRAKRTPKRAGIMIGLAW^{155}

IC3

C5aR ^{222}YTFILLRT*W*SR--------RA*T*RS*T*KTLK-VVVAVVASF^{251}
Rhod ^{223}YGQ**LVFTVKEAAAQQQESATTQKA**EKEVTRMVIIMVIAF^{261}
m5R ^{213}YCRIYRETEKRTK****KRVVLVKERKAAQTLSAILLAF^{451}

Ctail

C5aR ^{296}N*P*IIYVVAGQ*G*FQGRLRK*S*LPS^{317}
Rhod ^{302}NPVIY**IMMNKQFRNCMVTTLCC**^{323}
m5R ^{491}NPICYALCNRTFRKTFKMLLLC^{512}

FIGURE 11. **Comparison of preserved residues in the C5aR, rhodopsin, and the m5 muscarinic acetylcholine receptor.** Alignments of the intracellular loop regions and the flanking TM helices of the C5aR, rhodopsin (*Rhod*), and the m5 muscarinic acetylcholine receptor (*m5R*) are shown. Loop regions for rhodopsin as defined by the crystal structure (3) are shown in *bold*. The TM7 proximal regions of the carboxyl tails (*Ctail*) are shown. Residues essential for signaling in rhodopsin (8, 14, 17, 51–53) and the m5R (25–27) have been *underlined*. For the C5aR, these have been expanded to include preserved residues found in our previous TM screens (32, 33) (*underlined*) as well as other studies (55) (*italics*). For the IC3 loop of the m5 muscarinic receptor (~230 amino acids), only the amino- and carboxyl-terminal regions are shown, with the omitted residues indicated by *asterisks*. Residue positions in each receptor are indicated (*left* and *right*).

ies demonstrate a role for direct interactions between the receptor and G$\beta\gamma$ subunits (72–74). Therefore, stronger signaling may reflect the effects of mutations that optimize interactions between the human C5aR and the yeast G$\beta\gamma$ subunits.

Third, some receptors may contain mutations that allow them to more readily form higher ordered oligomers, which recent studies on rhodopsin demonstrate can activate G proteins much more efficiently than monomers and dimers (75). Our previous studies using fluorescence resonance energy transfer on the C5aR expressed in yeast demonstrated that the receptors do form oligomers (76), and disulfide trapping studies on the C5aR expressed in mammalian cells provided evidence for larger order oligomers (77).

Lastly, it is possible that selection of receptors with enhanced signaling ability may reflect removal of negative regulatory interactions within the receptor. For example, some residues in the intracellular loops of the wild-type C5aR may participate in interactions within and/or between the loops that help stabilize the receptor in the off-state. Mutation of stabilizing residues could interrupt these interactions, allowing the loop(s) to adopt a more open conformation that facilitates binding of G proteins. This may also prevent or hinder the return of the receptor to the basal state, thereby shifting the equilibrium toward the activated state. Ligand activation would then result in more persistent receptor activation. This has also been observed in extracellular loop 2 in the form of constitutively active C5aRs (29) and in the TM bundle in the form of residues that are evolutionarily conserved but not preserved in the genetic screens of the C5aR (29, 32, 33).

When the residues important for signaling identified in our screens are mapped on the three-dimensional structure of our C5aR model we see that the preserved residues cluster in the TM3 helix, the adjoining IC2 loop, the IC3 loop, and the adjoining TM6 helix (Fig. 10*b*). Interestingly, it has been demonstrated by EPR studies on rhodopsin that TM3 and TM6 show the largest intramolecular movement upon receptor activation and that this movement is required for G protein activation (78, 79). A similar movement of TM3 relative to TM6 has been suggested for the C5aR and other GPCRs (80, 81). We therefore propose that these residues create an activation face on the intracellular surface of the C5aR that participates in the initial interaction with G proteins and, consequently, in transmission of the conformational changes of the receptor to G proteins upon activation. To further understand how these residues activate G proteins, a docked structure of the receptor-G protein interaction will be required.

Acknowledgments—We thank members of the Baranski laboratory and Dr. Krzysztof Palczewski for helpful discussions and for review of the manuscript.

REFERENCES

1. Miller, K. J., Murphy, B. J., and Pelleymounter, M. A. (2004) *Curr. Drug. Targets CNS Neurol. Disord.* **3,** 357–377
2. Wess, J. (1998) *Pharmacol. Ther.* **80,** 231–264
3. Palczewski, K., Kumasaka, T., Hori, T., Behnke, C. A., Motoshima, H., Fox, B. A., Le Trong, I., Teller, D. C., Okada, T., Stenkamp, R. E., Yamamoto, M., and Miyano, M. (2000) *Science* **289,** 739–745
4. Teller, D. C., Okada, T., Behnke, C. A., Palczewski, K., and Stenkamp, R. E. (2001) *Biochemistry* **40,** 7761–7772
5. Okada, T., Fujiyoshi, Y., Silow, M., Navarro, J., Landau, E. M., and Shichida, Y. (2002) *Proc. Natl. Acad. Sci. U. S. A.* **99,** 5982–5987
6. Li, J., Edwards, P. C., Burghammer, M., Villa, C., and Schertler, G. F. (2004) *J. Mol. Biol.* **343,** 1409–1438
7. Okada, T., Sugihara, M., Bondar, A. N., Elstner, M., Entel, P., and Buss, V. (2004) *J. Mol. Biol.* **342,** 571–583
8. Franke, R. R., Sakmar, T. P., Graham, R. M., and Khorana, H. G. (1992) *J. Biol. Chem.* **267,** 14767–14774
9. Ernst, O. P., Hofmann, K. P., and Sakmar, T. P. (1995) *J. Biol. Chem.* **270,** 10580–10586
10. Acharya, S., and Karnik, S. S. (1996) *J. Biol. Chem.* **271,** 25406–25411
11. Konig, B., Arendt, A., McDowell, J. H., Kahlert, M., Hargrave, P. A., and Hofmann, K. P. (1989) *Proc. Natl. Acad. Sci. U. S. A.* **86,** 6878–6882
12. Ridge, K. D., Zhang, C., and Khorana, H. G. (1995) *Biochemistry* **34,** 8804–8811
13. Farahbakhsh, Z. T., Ridge, K. D., Khorana, H. G., and Hubbell, W. L. (1995) *Biochemistry* **34,** 8812–8819
14. Yang, K., Farrens, D. L., Hubbell, W. L., and Khorana, H. G. (1996) *Biochemistry* **35,** 12464–12469
15. Cai, K., Klein-Seetharaman, J., Farrens, D., Zhang, C., Altenbach, C., Hubbell, W. L., and Khorana, H. G. (1999) *Biochemistry* **38,** 7925–7930
16. Klein-Seetharaman, J., Hwa, J., Cai, K., Altenbach, C., Hubbell, W. L., and Khorana, H. G. (1999) *Biochemistry* **38,** 7938–7944
17. Natochin, M., Gasimov, K. G., Moussaif, M., and Artemyev, N. O. (2003) *J. Biol. Chem.* **278,** 37574–37581
18. Conner, A. C., Simms, J., Howitt, S. G., Wheatley, M., and Poyner, D. R. (2006) *J. Biol. Chem.* **281,** 1644–1651
19. Cai, K., Itoh, Y., and Khorana, H. G. (2001) *Proc. Natl. Acad. Sci. U. S. A.* **98,** 4877–4882
20. Itoh, Y., Cai, K., and Khorana, H. G. (2001) *Proc. Natl. Acad. Sci. U. S. A.* **98,** 4883–4887
21. Liu, J., Conklin, B. R., Blin, N., Yun, J., and Wess, J. (1995) *Proc. Natl. Acad. Sci. U. S. A.* **92,** 11642–11646
22. Liu, J., and Wess, J. (1996) *J. Biol. Chem.* **271,** 8772–8778
23. Erlenbach, I., and Wess, J. (1998) *J. Biol. Chem.* **273,** 26549–26558
24. Kim, J. M., Hwa, J., Garriga, P., Reeves, P. J., RajBhandary, U. L., and Khorana, H. G. (2005) *Biochemistry* **44,** 2284–2292
25. Burstein, E. S., Spalding, T. A., Hill-Eubanks, D., and Brann, M. R. (1995) *J. Biol. Chem.* **270,** 3141–3146
26. Hill-Eubanks, D., Burstein, E. S., Spalding, T. A., Brauner-Osborne, H., and Brann, M. R. (1996) *J. Biol. Chem.* **271,** 3058–3065
27. Burstein, E. S., Spalding, T. A., and Brann, M. R. (1998) *J. Biol. Chem.* **273,** 24322–24327
28. Erlenbach, I., Kostenis, E., Schmidt, C., Serradeil-Le Gal, C., Raufaste, D., Dumont, M. E., Pausch, M. H., and Wess, J. (2001) *J. Biol. Chem.* **276,** 29382–29392
29. Klco, J. M., Wiegand, C. B., Narzinski, K., and Baranski, T. J. (2005) *Nat. Struct. Mol. Biol.* **12,** 320–326
30. Klco, J. M., Nikiforovich, G. V., and Baranski, T. J. (2006) *J. Biol. Chem.* **281,** 12010–12019
31. Hagemann, I. S., Narzinski, K. D., Floyd, D. H., and Baranski, T. J. (2006) *J. Biol. Chem.* **281,** 36783–36792
32. Baranski, T. J., Herzmark, P., Lichtarge, O., Gerber, B. O., Trueheart, J., Meng, E. C., Iiri, T., Sheikh, S. P., and Bourne, H. R. (1999) *J. Biol. Chem.* **274,** 15757–15765
33. Geva, A., Lassere, T. B., Lichtarge, O., Pollitt, S. K., and Baranski, T. J. (2000) *J. Biol. Chem.* **275,** 35393–35401
34. Klein, C., Paul, J. I., Sauve, K., Schmidt, M. M., Arcangeli, L., Ransom, J., Trueheart, J., Manfredi, J. P., Broach, J. R., and Murphy, A. J. (1998) *Nat. Biotechnol.* **16,** 1334–1337
35. Brown, A. J., Dyos, S. L., Whiteway, M. S., White, J. H., Watson, M. A., Marzioch, M., Clare, J. J., Cousens, D. J., Paddon, C., Plumpton, C., Romanos, M. A., and Dowell, S. J. (2000) *Yeast* **16,** 11–22
36. Nikiforovich, G. V., and Marshall, G. R. (2005) *Biophys. J.* **89,** 3780–3789
37. Nikiforovich, G. V., and Marshall, G. R. (2003) *Biochemistry* **42,** 9110–9120
38. Nikiforovich, G. V., Mihalik, B., Catt, K. J., and Marshall, G. R. (2005) *J. Pept. Res.* **66,** 236–248
39. Dunfield, L. G., Burgess, A. W., and Scheraga, H. A. (1978) *J. Phys. Chem.* **82,** 2609–2616
40. Nemethy, G., Pottle, M. S., and Scheraga, H. A. (1983) *J. Phys. Chem.* **87,** 1883–1887
41. Dayhoff, M. O., Schwartz, R. M., and Orcutt, B. C. (1978) in *Atlas of Protein Sequence and Structure* (Dayhoff, M. O., ed) pp. 345–352, National Biomedical Research Foundation, Washington, D. C.
42. Fauchere, J. L., Charton, M., Kier, L. B., Verloop, A., and Pliska, V. (1988) *Int. J. Pept. Protein Res.* **32,** 269–278
43. Chen, Q., and Konopka, J. B. (1996) *Mol. Cell Biol.* **16,** 247–257
44. Hicke, L., and Riezman, H. (1996) *Cell* **84,** 277–287
45. Ballon, D. R., Flanary, P. L., Gladue, D. P., Konopka, J. B., Dohlman, H. G., and Thorner, J. (2006) *Cell* **126,** 1079–1093
46. Spain, B. H., Koo, D., Ramakrishnan, M., Dzudzor, B., and Colicelli, J. (1995) *J. Biol. Chem.* **270,** 25435–25444
47. Marion, S., Oakley, R. H., Kim, K. M., Caron, M. G., and Barak, L. S. (2006) *J. Biol. Chem.* **281,** 2932–2938
48. Moro, O., Lameh, J., Hogger, P., and Sadee, W. (1993) *J. Biol. Chem.* **268,** 22273–22276
49. Arora, K. K., Sakai, A., and Catt, K. J. (1995) *J. Biol. Chem.* **270,** 22820–22826
50. Smit, M. J., Roovers, E., Timmerman, H., van de Vrede, Y., Alewijnse, A. E., and Leurs, R. (1996) *J. Biol. Chem.* **271,** 7574–7582
51. Franke, R. R., Konig, B., Sakmar, T. P., Khorana, H. G., and Hofmann, K. P. (1990) *Science* **250,** 123–125
52. Acharya, S., Saad, Y., and Karnik, S. S. (1997) *J. Biol. Chem.* **272,** 6519–6524
53. Franke, R. R., Sakmar, T. P., Oprian, D. D., and Khorana, H. G. (1988) *J. Biol. Chem.* **263,** 2119–2122
54. Strader, C. D., Fong, T. M., Tota, M. R., Underwood, D., and Dixon, R. A. (1994) *Annu. Rev. Biochem.* **63,** 101–132
55. Kolakowski, L. F., Jr., Lu, B., Gerard, C., and Gerard, N. P. (1995) *J. Biol. Chem.* **270,** 18077–18082
56. Schulein, R., Hermosilla, R., Oksche, A., Dehe, M., Wiesner, B., Krause, G., and Rosenthal, W. (1998) *Mol. Pharmacol.* **54,** 525–535
57. Krause, G., Hermosilla, R., Oksche, A., Rutz, C., Rosenthal, W., and Schulein, R. (2000) *Mol. Pharmacol.* **57,** 232–242
58. Bermak, J. C., Li, M., Bullock, C., and Zhou, Q. Y. (2001) *Nat. Cell Biol.* **3,** 492–498
59. Pankevych, H., Korkhov, V., Freissmuth, M., and Nanoff, C. (2003) *J. Biol. Chem.* **278,** 30283–30293
60. Duvernay, M. T., Zhou, F., and Wu, G. (2004) *J. Biol. Chem.* **279,** 30741–30750
61. Robert, J., Clauser, E., Petit, P. X., and Ventura, M. A. (2005) *J. Biol. Chem.* **280,** 2300–2308
62. Estall, J. L., Koehler, J. A., Yusta, B., and Drucker, D. J. (2005) *J. Biol. Chem.* **280,** 22124–22134
63. Thielen, A., Oueslati, M., Hermosilla, R., Krause, G., Oksche, A., Rosenthal, W., and Schulein, R. (2005) *FEBS Lett.* **579,** 5227–5235
64. Giannini, E., Brouchon, L., and Boulay, F. (1995) *J. Biol. Chem.* **270,** 19166–19172
65. Giannini, E., and Boulay, F. (1995) *J. Immunol.* **154,** 4055–4064
66. Naik, N., Giannini, E., Brouchon, L., and Boulay, F. (1997) *J. Cell Sci.* **110,** 2381–2390
67. Christophe, T., Rabiet, M. J., Tardif, M., Milcent, M. D., and Boulay, F. (2000) *J. Biol. Chem.* **275,** 1656–1664
68. Braun, L., Christophe, T., and Boulay, F. (2003) *J. Biol. Chem.* **278,**

4277–4285
69. Auger, G. A., Smith, B. M., Pease, J. E., and Barker, M. D. (2004) *Immunology* **112,** 590–596
70. von Heijne, G. (1992) *J. Mol. Biol.* **225,** 487–494
71. Filipek, S., Krzysko, K. A., Fotiadis, D., Liang, Y., Saperstein, D. A., Engel, A., and Palczewski, K. (2004) *Photochem. Photobiol. Sci.* **3,** 628–638
72. Kisselev, O., and Gautam, N. (1993) *J. Biol. Chem.* **268,** 24519–24522
73. Kisselev, O. G., Ermolaeva, M. V., and Gautam, N. (1994) *J. Biol. Chem.* **269,** 21399–21402
74. Kisselev, O., Ermolaeva, M., and Gautam, N. (1995) *J. Biol. Chem.* **270,** 25356–25358
75. Jastrzebska, B., Fotiadis, D., Jang, G. F., Stenkamp, R. E., Engel, A., and Palczewski, K. (2006) *J. Biol. Chem.* **281,** 11917–11922
76. Floyd, D. H., Geva, A., Bruinsma, S. P., Overton, M. C., Blumer, K. J., and Baranski, T. J. (2003) *J. Biol. Chem.* **278,** 35354–35361
77. Klco, J. M., Lassere, T. B., and Baranski, T. J. (2003) *J. Biol. Chem.* **278,** 35345–35353
78. Farrens, D. L., Altenbach, C., Yang, K., Hubbell, W. L., and Khorana, H. G. (1996) *Science* **274,** 768–770
79. Sheikh, S. P., Zvyaga, T. A., Lichtarge, O., Sakmar, T. P., and Bourne, H. R. (1996) *Nature* **383,** 347–350
80. Sheikh, S. P., Vilardarga, J. P., Baranski, T. J., Lichtarge, O., Iiri, T., Meng, E. C., Nissenson, R. A., and Bourne, H. R. (1999) *J. Biol. Chem.* **274,** 17033–17041
81. Gerber, B. O., Meng, E. C., Dotsch, V., Baranski, T. J., and Bourne, H. R. (2001) *J. Biol. Chem.* **276,** 3394–3400
82. Matsumoto, M. L., Narzinski, K., Nikiforovich, G. V., and Baranski, T. J. (2007) *J. Biol. Chem.* **282,** 3122–3133